A Simplified Shear Design Method For Post Tensioned Concrete

A THESIS
SUBMITTED TO THE FACULTY OF THE
UNIVERSITY OF MINNESOTA
BY

Dalton J. Scharmer

IN PARTIAL FULFILLMENT OF THE REQUIREMENTS
FOR THE DEGREE OF MASTER OF SCIENCE

DR. ANDREA SCHOKKER

September 2022

Acknowledgements

First, I would like to thank all the UMD faculty, especially those within the civil engineering department for their continued support through my educational career. A special thank you to Dr. Andrea Schokker for going above and beyond what I expected any advisor to do for me, and to Dr. Ben Dymond and Dr. Alison Hoxie for serving on my committee. Additionally, I would like to thank my fellow graduate students: Tim Clemet, Kendall Hill, Austin Janson, Alex Kulzer, Vishruthi Manickavasagan, and Pranav Sharma for keeping the culture lively in the office and making graduate school so enjoyable.

Second, I would like to thank my siblings: Audrey Meyer, Brittany McNallan, Courtney Scharmer, Ethan Scharmer, and my parents: Jenny and Tim Scharmer, for helping support me through school and encouraging me to chase my dreams. The steady love and support from my family has helped me through all the trials and tribulations school and life has thrown at me over these past five years of higher education. Also, to my adopted family of roommates: Trent Brunner, Sam Carman, Alex Chapman, Elliot Habel, Adam Hogquist, Michael Messenger, Trevor Raths, Preston Reed, and Nick Schmidt thank you for all the support throughout our time living with each other. I consider you all family and look back on our time together very fondly.

Next, I would like to thank everyone at the UMD Newman center, especially Neal Anderson, Sam Carlson, Fr. Mike Schmitz, Heather Serena, and Alex Wilde, for walking with me as I discovered and continue to learn the reason to pursue excellence in every part of my life and who Jesus Christ is. My life has completely changed, and I am not only a better engineer, but also a better man because of this community.

Finally, I give thanks and glory to God for showing me my purpose in this world and blessing me in more ways than I can count. For apart from Him, I can do nothing. Everything I am, and do, is in the name of Jesus Christ and for the expansion of God's kingdom.

Abstract

Shear forces are one of the primary forces that need to be accounted for when designing a prestressed, post tensioned, or regular reinforced concrete member. Shear forces can cause brittle, and often disastrous failure if a section is not properly designed. The ACI 318-19 code has several methods for calculating the nominal capacity of various concrete members. This research project considers the current code equations for prestressed concrete, and a new modified version of the equation for non-prestressed members that allows unification of concrete shear design as an alternate simplified method.

The goal of this project is to evaluate a more straight-forward shear design approach for post-tensioned members. The detailed method used in pretensioned members models the effects of inclined and web shear types of failures reasonably well for determinate members. However, the typical post-tensioned member is often indeterminate with a series of parabolic tendon profiles and is more complicated to model with potentially little gain in reducing stirrup requirements. A basic approach that is similar to the new non-prestressed equations in ACI 318-19 is provided as an alternate method. While the proposed method would be a conservative option for pretensioned members, the likely application is in continuous post-tensioned members.

Table of Contents

Chapter 1: Introduction

1.1 Background

All concrete members must be able to handle a certain design load based on the intended use of the concrete member. The magnitude of the design load is determined by looking at a variety of loading combinations stated in section 5.3 of ACI 318 (2019), *Building Code Requirements for Structural Concrete.* These load combinations are the standard for strength requirements of all concrete members and the design load is taken as the greatest of all the load combinations. Once the design load is determined, the concrete member is designed for strength and serviceability. This research focuses on one-way shear in prestressed beams; therefore, this will be the focus on the literature review and background. As flexural members, beams are designed for ductile behavior in bending with appropriate shear reinforcement to ensure that the section does not fail in shear.

Shear strength and behavior has been the focus of much research for both prestressed and non-prestressed concrete members. While designing and producing strong and safe concrete members is essential for the safety of the public, there is also the realization that these concrete members must be as efficient as possible to minimize their environmental impact and stay economically competitive in the building materials market. Finding the balance between safety and efficiency within concrete members can be a difficult task. Pretensioned precast concrete (PS/PC) and post-tensioned (PT) concrete have proven to be more efficient and durable in many applications than traditionally reinforced concrete (RC). The current ACI 318-19 code treats non-prestressed and prestressed members separately; that is, there is not a unified approach to shear. More details regarding the different methods and the challenges will be provided in Chapter 2.

Shear failures are a significant concern because they often happen suddenly and can be catastrophic. The design shear strength for PS concrete is determined by using one of two main sets equations found in ACI 318 (2019), *Building Code Requirements for Structural Concrete.* The shear capacity (V_n) of the concrete member is expressed as the summation of the concrete shear strength (V_c) and reinforcement shear strength (V_s) before

being multiplied by a safety factor (Ø) of 0.75. This total must be greater than the factored shear demand (V_u). The concrete shear strength component (V_c) is the focus of this work.

1.1 Thesis Organization

Chapter 2 provides an in-depth look at past and current design equations, summarizes the terminology associated with them, and states the main focus of this thesis. Chapter 3 introduces and discusses the methods in developing the proposed equation for post-tensioned members and provides two examples that were used in the research. Chapter 4 discusses the results of the proposed method compared to current code equations. Chapter 5 presents the conclusions and recommendations for future work following the experiment.

Chapter 2: Literature Review

2.1 Notation

The following is a summary of the variables used within the ACI, and other code equations. If a variable represents something differently than expressed in this section (the meanings have changed over time) then it will be explicitly stated when the equation is referenced.

$A_g =$ gross area of concrete section, in^2 for a hollow section, A_g is the area of the concrete only and does not include the area of the void(s)

$A_{ps} =$ area of prestressed longitudinal tension reinforcement, in^2

$A_s =$ area of nonprestressed longitudinal tension reinforcement, in^2

$A_v =$ area of shear reinforcement within spacing s, in^2

$A_{v,min} =$ minimum area of shear reinforcement within spacing s, in^2

$b_w =$ web width or diameter of circular section, in

$d =$ distance from extreme compression fiber to centroid of longitudinal tension reinforcement, in

$d_e =$ effective depth from extreme compression fiber to the centroid of the tensile force in the tensile reinforcement

$d_p =$ distance from extreme compression fiber to centroid of prestressed reinforcement, in

$d_v =$ effective shear depth taken as the distance, measured perpendicular to the neutral axis, between the resultants of the tensile and compressive forces due to flexure; it need not be taken to be less than the greater of 0.9de or 0.72h

$f_c' =$ specified compressive strength of concrete, psi

$f_d =$ stress due to unfactored dead load, at extreme fiber of section where tensile stress is caused by externally applied loads, psi

f_{pc} = compressive stress in concrete, after allowance for all prestress losses, at centroid of cross section resisting externally applied loads or at junction of web and flange where the centroid lies within the flange, psi. In a composite member, f_{pc} is the resultant compressive stress at centroid of composite section, or at junction of web and flange where the centroid lies within the flange, due to both prestress and moments resisted by precast member acting alone

f_{pe} = compressive stress in concrete due only to effective prestress forces, after allowance for all prestress losses, at extreme fiber of section if tensile stress is caused by externally applied loads, psi

f_{pu} = specified tensile strength of prestressing reinforcement, psi

f_{se} = effective stress in prestressed reinforcement, after allowance for all prestress losses, psi

f_y = yield stress of stirrups

N_u = factored axial force normal to cross section occurring simultaneously with Vu or Tu; to be taken as positive for compression and negative for tension, lb

m = Constant used to calibrate proposed equation in parametric study

M_{cre} = moment causing flexural cracking at section due to externally applied loads, in.-lb

M_{max} = maximum factored moment at section due to externally applied loads, in.-lb

M_u = factored moment at section, in.-lb

P = Prestressing force, lb

s = center-to-center spacing of items, such as longitudinal reinforcement, transverse reinforcement, tendons, or anchors, in.

V_n = nominal shear strength, lb

v_c = concrete contributions when the shear stress causes diagonal cracking (v_{cr}), psi

v_{cr} = shear stress that causes diagonal cracking, psi

V_c = design shear force for load combinations including earthquake effects, lb

V_{ci} = nominal shear strength provided by concrete where diagonal cracking results from combined shear and moment, lb

V_{cw} = nominal shear strength provided by concrete where diagonal cracking results from high principal tensile stress in web, lb

V_d = shear force at section due to unfactored dead load, lb

V_i = factored shear force at section due to externally applied loads occurring simultaneously with M_{max}, lb

V_n = Nominal Shear Capacity, lb

V_p = vertical component of effective prestress force at section, lb

V_s = nominal shear strength provided by shear reinforcement, lb

V_u = factored shear force at section, lb

λ = modification factor to reflect the reduced mechanical properties of lightweight concrete relative to normal weight concrete of the same compressive strength

λ_s = factor used to modify shear strength based on the effects of member depth, commonly referred to as the size effect factor.

ρ_w = ratio of A_s to b_w*d

ρ_z = ratio of stirrups area to the web area

Υ_d = size effect factor

Ø = Strength Reduction Factor

2.2 Current Building Codes and Standards

2.2.1 ACI 318 Building Code Requirements for Structural Concrete (2019)

ACI 318 (2019) provides the governing equations that standardize the design of concrete structures. Designed to handle various types of members (ex. PS and RC concrete) and different stresses in the members (ex. flexure and shear), ACI 318 (2019) equations govern the design of buildings and other similar concrete structures. The shear design

equations have been modified over time, and some new literature suggests additional changes may be advantageous, particularly in light of the development of two new codes to address specifically precast concrete (ACI 319) and post-tensioned concrete (ACI 320) for publication in 2025. Equations in this section are labeled to reflect if they are historical, current, or proposed equations throughout this research project.

Shear design is most generally summarized by the following equations.

$$V_n = V_c + V_s \qquad \text{ACI 22.5.1.1}$$

$$\emptyset V_n \geq V_u \qquad \text{Eq. 2.2.1A}$$

Where:

$$V_u \leq \emptyset(V_c + 8\sqrt{f_c'} b_w d) \qquad \text{ACI 22.5.1.2}$$

$\emptyset = 0.75$

ACI 22.5.1.1 states that the shear strength of a concrete member is simply the summation of the concrete shear strength (V_c) and the steel contribution to shear strength (V_s). V_s is gained by adding stirrups to the concrete member; however, some pretensioned concrete members such as hollow core planks cannot contain stirrups due to their geometric and construction process constraints. Other sections such as double tees use mesh reinforcement only in the ends of the span. Without being able to add stirrups (and thus reducing V_s to zero) some concrete members must solely rely on the concrete shear strength, V_c, to meet the shear demand on the structure (V_u). The code requires a factor of 2 times V_c for members without shear reinforcement. Additionally, there is an upper limit to how much shear stress the cross-section of the concrete is allowed to carry. If ACI 22.5.1.2 is not satisfied, then the section must be redesigned to provide the minimum required strength from the concrete portion.

ACI 22.5.5.1 lists three different equations for determining V_c for RC members, which is summarized in table 2.2.1B below. By following table 2.2.1B, determining V_c is straightforward.

Criteria	V_c		
$A_v \geq A_{v,min}$	Either of:	$\left[2\lambda\sqrt{f_c'} + \frac{N_u}{6A_g}\right] b_w d$	(a)
		$\left[8\lambda(\rho_w)^{1/3}\sqrt{f_c'} + \frac{N_u}{6A_g}\right] b_w d$	(b)
$A_v < A_{v,min}$	$\left[8\lambda_s\lambda(\rho_w)^{1/3}\sqrt{f_c'} + \frac{N_u}{6A_g}\right] b_w d$		(c)

Table 2.2.1B: V_c for Nonprestressed Members

Where:

$\frac{N_u}{6*A_g} \leq 0.05 f_c'$ ACI 18-19 22.5.5.1.2

$\lambda_s = \sqrt{\frac{2}{1+\frac{d}{10}}} \leq 1$ ACI 18-19 22.5.5.1.3

Once V_c is determined from table 2.2.1B, it must be checked against an upper bound. The final check for determining V_c is listed below in ACI 18-19 22.5.5.1.1

$$V_c \leq 5\,\lambda\sqrt{f_c'} b_w d \qquad \text{ACI 18-19 22.5.5.1.1}$$

ACI 22.5.6.2 provides two shear design methods for PS flexural members: the simplified and detailed methods. V_c for the simplified method of a member is to be taken

as the minimum of equations 22.5.6.2a, 22.5.6.2b and 22.5.6.2c (MacGregor and Hanson 1969). These equations are only applicable for prestressed beams or beams with both prestressing reinforcement and non-prestressed reinforcement.

$$\left(0.6\lambda\sqrt{f_c'} + 700\frac{V_c d_p}{M_u}\right) b_w d \qquad \text{ACI 318-19 22.5.6.2a}$$

$$\left(0.6\lambda\sqrt{f_c'} + 700\right) b_w d \qquad \text{ACI 318-19 22.5.6.2b}$$

$$5\lambda\sqrt{f_c'} b_w d \qquad \text{ACI 318-19 22.5.6.2c}$$

In most situations the simplified method provides an adequate design strength; however, it may be unconservative in some situations when the beam is deep. This is known as the size effect factor (Υ_d), which will be explained later in this section.

ACI also includes a method for determining shear strength that includes different terms for V_c depending on the type of cracking that controls along the span of a concrete member. This is commonly referred to as the detailed method or V_{ci}, V_{cw} method. The detailed method for calculating V_c is to take the minimum of the equations for flexure-shear (V_{ci}) and web-shear (V_{cw}). The theory behind the development of V_{ci} and V_{cw} is discussed in section 2.3.2.

$$V_c = minimum\ (V_{ci}\ , V_{cw}) \qquad \text{Eq 2.2.1C}$$

$$V_{ci} = 0.6\lambda\sqrt{f_c'} b_w d_p + V_d + \frac{V_i M_{cre}}{M_{max}} \qquad \text{ACI 18-19 22.5.6.3.1}$$

$$V_{cw} = \left(3.5\lambda\sqrt{f_c'} + 0.3\ f_{pc}\right) b_w d_p + V_p \qquad \text{ACI 18-19 22.5.6.3.2}$$

Where:

$$M_{cre} = \frac{1}{y_t}\ (6\lambda\sqrt{f_c'} + f_{pe} - f_d) \qquad \text{ACI 18-19 22.5.6.3.1d}$$

For members with $A_{ps} f_{se} < 0.4\left(A_{ps} f_{pu} + A_s f_y\right)$

$$V_{ci} \geq 2\lambda\sqrt{f_c'} b_w d \qquad \text{ACI 18-19 22.5.6.3.1b}$$

For members with $A_{ps}f_{se} \geq 0.4\left(A_{ps}f_{pu} + A_s f_y\right)$

$$V_{ci} \geq 2\lambda\sqrt{f_c'}b_w d \qquad \text{ACI 18-19 22.5.6.3.1c}$$

The detailed method for determining the V_c is more complicated than the simplified method, but it more accurately represents the behavior of prestressed members in shear. Since V_c is typically controlled by V_{ci} near the middle of the beam and V_{cw}typically controls near the ends of the span, the resulting plot for the concrete strength is discontinuous where the equations intersect.

2.3 Historical Evolution of Shear

Shear design equations in the ACI 318 code have been in development for well over 50 years. The most basic understanding for shear design equations is that a RC member gains strength from the concrete (V_c) and any shear reinforcement (V_s) it has. The conservative nature of these equations is essential due to the severity of a shear failure within concrete. The literature review analyzed many journal articles focusing on the revision of, at the time, current design equations, and attempting to improve upon them. An overview based on Collins and Kuchma (1999) and Saqan and Frosh (2009) is outlined in the following paragraphs.

In 1962, ACI-ASCE committee 326 reported that the basic expression for diagonal cracking sheer, V_c, did not account for effects of reinforcement ratio or cross-section size. The equation, listed below, becomes much less conservative when applied to large members with small percentages of reinforcement.

$$V_c = 2\sqrt{f_c'}b_w d \qquad \text{Eq2.3A}$$

This equation was a significant factor in shear reinforcement design until ACI-ASCE committee 326 did a major review of the equation in 1962 following the partial collapse of the Wilkins Air Force Depot resulting from a shear failure in a 36-inch-deep beam. This beam did not contain any stirrups for additional reinforcement (no V_s), had a

longitudinal reinforcement ratio of 0.45%, and was only subjected to 83% of its design capacity of the time. After completing a series of experiments on different beams, they determined that the addition of an axial tensile stress reduced the shear capacity by about 50%. This experiment led to the conclusion that the beams at the Wilkins Air Force Depot failed because the shrinkage and thermal movements of the concrete induced an axial tensile stress and therefore reduced the shear capacity. More research on this topic was done in 1967 by Kani that clearly demonstrates the negative correlation between the depth of a beam and the shear stress at failure (this is the first introduction to the size effect factor, Υ_d). A negative effect on shear capacity when combined with a tensile axial load was found through this research project; however, due to issues with testing, none of these beams failed at less than the original V_c equation predicted. Therefore, no change was made to the ACI code.

As testing continued, it was determined that the size effect created up to a 50 percent reduction in the failure shear stress between models and prototypes of the Air Force warehouse beams. The unconservative nature of these large beams is mitigated in the ACI code due to the requirement for minimum stirrups to be provided whenever the factored shear force exceeds $0.5\emptyset V_c$.

A new methodology for calculating shear reinforcement in concrete bridge members called the "modified compression field theory" was introduced in 1994 in the bridge design code (AASHTO LRFD Design Specifications and Commentary) and the Canadian standard for the "Design of Concrete Structures" (CSA Committee 1994). This method assumes that shear strength can be determined as a function of crack length and crack spacing. The hypothesis is that since the crack spacing is related to the strain in the longitudinal reinforcement, the larger members will fail at a lower shear strength.

As the experimental data and design philosophies surrounding concrete continued to evolve (ex. prestressing), the equations used to predict the shear capacity of these members had to change to reflect the improved performance of these members.

2.3.1 45-Degree Truss Model and Modified Compression Field Theory (MCFT)

The 45- Degree Truss Model is one of the oldest shear design procedures, going back more than 100 years. The 45-Degree Truss Model states that shear stress is solely resisted by cracked concrete in the web of a beam. The stresses in the concrete member were thought to be applied at a 45-degree angle to the longitudinal axis of the concrete member. For concrete members with flanges, these diagonal forces were thought to cause tension in the stirrups of the member by pushing apart the flanges. This method ignores the tensile strength of concrete; therefore, it is conservative by nature, especially in members with small amounts of stirrups. While the 45-Degree Truss Model represents behavior in a non-prestressed member reasonably well, the angle can be considerably shallower in prestressed members (Solanki 2007).

The shear strength of the concrete members increased when a term was added to account for prestressing force. After this change (beginning in the 1970s), European researchers began experimenting to determine if there was a more accurate value for the angle of the diagonal compressive stresses in the web (θ) which at the time were assumed to be 45 degrees. Models based on the theory of plasticity and strain in the web of the concrete members resulted in the evidence to support that the shear angle of these cracks could be much smaller than the original 45 degrees for prestressed concrete. Some lower limits were put in place (ex. $\theta > 30$ degrees) but decreasing the angle of the force reduced the strain in the prestressing tendons and increased the design shear strength within the section. This improved theory was termed the Compression Field Theory (CFT). After Vecchio and Collins discovered that tensile stresses were still present between cracks in concrete, they made some slight modifications of the CFT to create the Modified Compression Field Theory (MCFT) (Vecchio, Collins 1982).

The MCFT was designed for determining the shear capacity of a concrete member given a few basic physical characteristics such as the factor for tensile stress in cracked concrete, β, and the crack angle, θ. The MCFT assumptions and equations are summarized in the figure below. A spreadsheet or other software is often used in practice for these calculations.

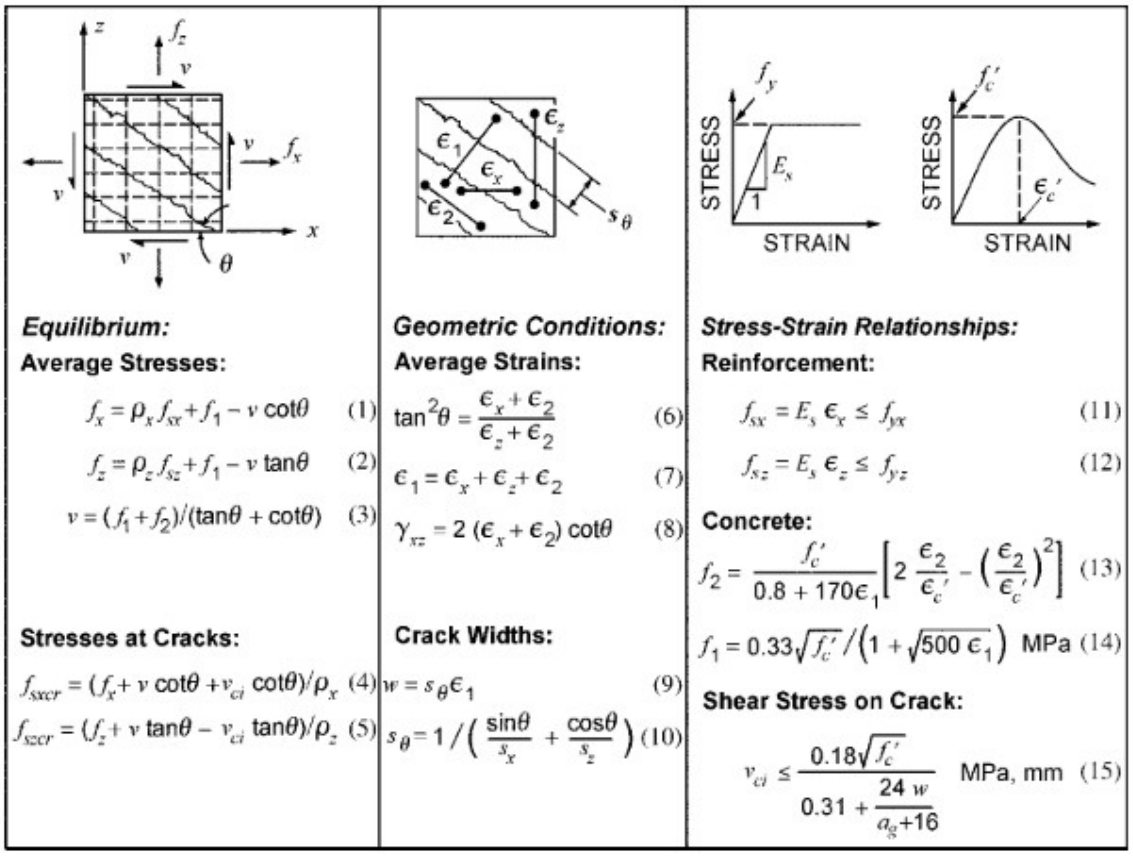

Figure 2.3.1A: Summary of MCFT equations **(**Solanki 2007)

2.3.2 Current Shear Design Procedure for Prestressed Members (Detailed Method)

The current ACI equations that are used to determine concrete shear capacity for prestressed members are the cumulation of decades worth of research. When designing for shear strength (V_c) of a concrete member, there are typically two different shear failure modes that control the design strength: web-shear (V_{cw}) and flexure-shear (V_{ci}). Web-shear (V_{cw}) failures are caused due to high principal tensile stresses in the web of the concrete member. This failure is typically seen near the supports of the concrete member. The MCFT was used to derive the web-shear equation. Flexure-shear, also known as inclined shear, (V_{ci}) failures are caused by combined shear and moments applied to the member

(Perumalla, Yogeendra 2022; Kang, Lee, Yerzhanov, Ju 2021). This failure controls near the center of the concrete member because that is where flexure dominates the stress distribution. V_c is determined to be the minimum of V_{cw} and V_{ci} and changes based on the location of the beam that is being analyzed. This means V_{cw} and V_{ci} must be computed for the entire length because the controlling capacity changes between the two equations throughout the beam. Once V_c is determined, the next steps in the design process are to multiply it by a strength reduction factor (Ø) of 0.75. $\emptyset = 0.75$ is the standard value for shear reinforcement due to the severity and sudden nature of shear failures. After determining $\emptyset V_c$, the two equations below determine if the section needs to be revised, needs stirrups, or if it doesn't need stirrups.

$$\frac{V_u}{\emptyset} - V_c \leq 8\sqrt{f_c'} b_w d \qquad \text{ACI 22.5.1.2}$$

$$V_u \leq 0.5 * \emptyset V_c \qquad \text{Eq 2.3.2A}$$

If ACI 22.5.1.2 fails, the concrete member will not work and needs to be redesigned. If ACI.22.5.1.2 and equation 2.3.2A pass, the concrete member has enough shear capacity from the concrete contribution alone that it does not need any stirrups added for shear strength. If ACI 22.5.1.2 passes, but the equation 2.3.2A fails, the concrete member will still work, but will need additional shear strength (V_s) in the form of stirrups.

Adding stirrups to concrete sections is very common. They provide additional shear reinforcement and can help with the constructability of rebar cages. Typically, #3, #4 or #5 rebars are used for stirrups because large diameter bars are difficult to bend, and large diameter bars will raise the position of the flexural reinforcement higher into the member. Once a bar size is chosen, a spacing (s) of the stirrups must be determined. There is also minimum steel ($A_{v,\min}$) requirements, and maximum spacing consideration when designing a concrete member for shear reinforcement. Minimum steel requirements and maximum spacing provisions are intended to help control cracking. The equations for the maximum spacing were derived considering the 45-Degree Truss Model, MCFT, and the angle cracks typically follow in concrete members. If spaced properly, no crack the

concrete member experiences would be able to go from the bottom of the member to the top without crossing paths with at least one stirrup, which should help prevent a crack from worsening. The following equations summarizes the final steps of the detailed method.

$$s = \frac{A_v * f_y * d}{\frac{V_u}{\emptyset} - V_c} \quad \text{Eq 2.3.2B}$$

Where:

$$A_v = 2 * stirrup\ diameter \quad \text{Eq 2.3.2C}$$

$$A_{v1} = 0.75 * \sqrt{f_c'}\,\frac{b_w * s}{f_y}\ but\ not\ less\ than\ \frac{50 * b_w * s}{f_y} \quad \text{Eq 2.3.2D}$$

$$A_{v2} = \frac{A_{ps}}{80} * \frac{f_{pu}}{f_y} * \frac{s}{d}\sqrt{\frac{d}{b_w}} \quad \text{Eq 2.3.2E}$$

$$A_{v,min} = \min(A_{v1}, A_{v2}) \quad \text{Eq 2.3.2F}$$

$$A_v > A_{v,min} \quad \text{Eq 2.3.2G}$$

$$V_s = \frac{A_v * f_y * d}{s} \quad \text{Eq 2.3.2H}$$

If:

$$V_s \geq 4 * \sqrt{f_c'} * b_w * d \quad \text{Eq 2.3.2I}$$

$$s_{max} = \min(0.375 * h\,, 12) \quad \text{Eq 2.3.2J}$$

If:

$$V_s < 4 * \sqrt{f_c'} * b_w * d \quad \text{Eq 2.3.2K}$$

$$s_{max} = \min(0.75 * h\,, 24) \quad \text{Eq 2.3.2L}$$

The iterative design process, while time consuming, is relatively straightforward with the aid of a spreadsheet or software. Constructability is also considered in terms of spacing consistency and precision. While these aren't addressed in the code explicitly, they should be considered when designing concrete members.

2.3.3 Post-Tensioning Shear

Pretensioned precast members are typically simply supported, determinant members, but post-tensioned members are often continuous structures that span multiple supports and are structurally indeterminant. Indeterminate PT structures must consider secondary moments when evaluating their flexural design capacity. Typically, when concrete members are post-tensioned, the member will deflect up due to the effective prestress force; however, because of the redundant supports on these structures keeping the members from deflecting, there is an induced secondary moment. The figure below illustrates what a simply supported prestressed or post-tensioned beam looks like, and what a continuous beam looks like.

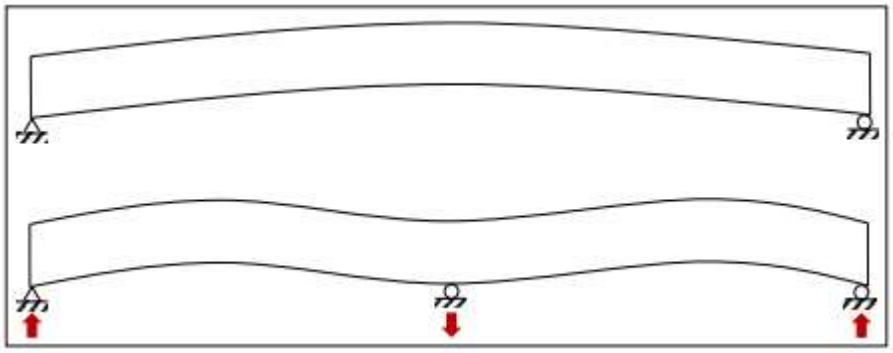

Figure 2.3.3A: Secondary Moment Diagram (Schokker 2018)

As shown in Figure 2.3.3A, the beam is held from upward deflection by the middle support when under the prestress force. This geometric constraint affects the reaction forces at the other supports and must be accounted for in the flexural design capacity.

Continuous structures are post-tensioned rather than pretensioned due to the ability for the post-tensioning tendons to take a parabolic shape that roughly follows the applied moment. One of the unique parts about analyzing these structures is that unlike in simply supported members where the bottom face of the member is typically always in tension once loaded, the tension face in continuous structures changes at inflection points between supports. This requires careful tracking of the compression face of the member when

analyzing and designing a post-tensioned member for shear, but the shear design process remains the same as for determinate members.

2.4 Additional Prestressed Shear Design Literature

While not every piece of academic literature reviewed for this thesis was directly cited in the discussion of the previous sections, several papers helped to develop the knowledge base upon which this thesis was written. Three main papers and their contributions to the literature are discussed in this section.

Proposals for New One-Way Shear Equations for the 318 Building Code **by Belarbi, Kuchma, and Sanders (2017)**

This paper begins by stating that there is a need to develop a new approach for one-way shear design. The paper first summarizes the history of design provisions from several researchers (Bentz, Collins 2017; Cladera, Marí, Bairán, Oller, Ribas, 2017; Frosch, Yu, Cusatis, Bažant 2017; Li 2017; Park, Choi 2017; Reineck 2017). Next, they mention how the 45-degree truss model was overly conservative and summarize the 17 different one-way shear provisions listed in the ACI 318-14 code in the table below.

ACI 318-14	Simplified method	Detailed method
V_n	$V_n = V_c + V_s$ $V_u \le \phi(V_c + 8\sqrt{f'_c}\, b_w d)$	
RC, V_c	$V_c = 2\lambda\sqrt{f'_c}\, b_w d$	Lesser of: $V_c = \left[1.9\lambda\sqrt{f'_c} + 2500\rho_w \frac{V_u d}{M_u}\right] b_w d$ $V_c = \left[1.9\lambda\sqrt{f'_c} + 2500\rho_w\right] b_w d$ $V_c = 3.5\lambda\sqrt{f'_c}\, b_w d$
V_c with axial load N_u	Axial compression: $V_c = 2\left[1 + \frac{N_u}{2000 A_g}\right]\lambda\sqrt{f'_c}\, b_w d$ Axial tension: $V_c = 2\left[1 + \frac{N_u}{500 A_g}\right]\lambda\sqrt{f'_c}\, b_w d$	Axial compression (lesser of): $V_c = \left[1.9\lambda\sqrt{f'_c} + 2500\rho_w \frac{V_u d}{M_m - N_u \frac{(4h-d)}{8}}\right] b_w d$ $V_c = 3.5\lambda\sqrt{f'_c} b_w d \sqrt{1 + \frac{N_u}{500 A_g}}$
PC, V_c	Lesser of (a), (b), and (c), but > (d): $V_c = \left[0.6\lambda\sqrt{f'_c} + 700\frac{V_u d_p}{M_u}\right] b_w d$ (a) $V_c = \left[0.6\lambda\sqrt{f'_c} + 700\right] b_w d$ (b) $V_c = 5\lambda\sqrt{f'_c} b_w d$ (c) $V_c = 2\lambda\sqrt{f'_c} b_w d$ (d)	Lesser of V_{ci} and V_{cw}: $V_{ci} = 0.6\lambda\sqrt{f'_c} b_w d_p + V_d + \frac{V_i M_{cre}}{M_{max}}$ or $1.7\lambda\sqrt{f'_c} b_w d$ (use largest) $V_{cw} = (3.5\lambda\sqrt{f'_c} + 0.3 f_{pc}) b_w d_p + V_p$
V_s	$V_s = \frac{A_v f_{yt} d}{s}$	

Table 2.4A: Summary of One-Way Shear Provisions

The authors then go on to discuss potential shortcomings of the design provisions. They also mention that while the shear data based used to derive these equations are useful, it cannot be the ultimate justification for design provisions because the data base has biases and limitations. The limitations that the authors address within the article are similar, if not the same issues that were considered during the drafting of this thesis. Primarily, the shear database contains members that are pretensioned with smaller spans and cross-sections due to lab testing limitations.

A Unified Approach to Shear Design **by Robert J Frosh, Qiang Yu, Gianluca Cusatis, and Zdeněk P. Bažant (2017)**

These authors start by stating that current design provisions were developed using specimens and technology that are now outdated. The members used to develop these equations had low percentages of flexural reinforcement, do not include high strength concrete members, and lack member size variety. The authors state that technological improvements of the materials used within the construction industry are paving the way for the industry to eliminate past practices and provide improved safety for our structures through the development of a unified design method.

With regards to the reinforcement ratio (ρ), the study found that as the reinforcement ratio increases, the current equations become more conservative. This positive correlation leads the authors to suggest that by considering the depth of the neutral axis rather than the depth of the tendon (d), the overly conservative nature of the old equation can be solved with the new V_{calc} equation listed below. This slight change keeps the conservative nature of the V_{calc} equation constant as the reinforcement ratio of the member increases. It also changes the constant in front of the $\sqrt{f_c'}$ term to fit the data set more accurately.

$$V_{calc} = 2\sqrt{f_c'}b_w d \qquad \text{Old Equation}$$

$$V_{calc} = 5\sqrt{f_c'}b_w c \qquad \text{New Equation}$$

After addressing the reinforcement ratio issue, the authors move to address the lack of need for limiting the upper bound of $\sqrt{\boldsymbol{f_c'}}$ to be less than 100 psi. Today, it is not uncommon for the compressive strength of concrete to exceed 10,000 psi. The increased strength and the calculated capacity that would be gained by dismissing the upper limit of $\sqrt{\boldsymbol{f_c'}}$ is shown in the paper to still be conservative.

Finally, the authors briefly discuss the size factor ($\Upsilon_{\mathbf{d}}$) of concrete members. If the reinforcement ratio is held constant, a doubling of the depth ($\boldsymbol{d}$) to the reinforcement does not equate to a doubling of the shear strength of the member. All these factors are summarized and concluded with the authors proposing the following concrete shear strength equation for one and two-way shear, followed by a simplified equation.

$$V_c = \left(5\lambda\sqrt{f_c'}b_w c\right)\ \Upsilon_{\mathrm{d}} \qquad V_c \text{ with Size Factor}$$

$$\mathrm{V_c}\ = 10\lambda\sqrt{\mathrm{f_c'}}\mathrm{b_o c} \qquad \text{Proposed Simplified}$$

Where:

$$\Upsilon_{\mathbf{d}} = \frac{\mathbf{1.4}}{\sqrt{\mathbf{1}+\boldsymbol{d_t}/\boldsymbol{d_0}}} \qquad \text{Eq 2.4B}$$

ACI 318 Shear Design Method for Prestressed Concrete Members **by Thomas Kang, Deuckhang Lee, Meirzhan Yerzhanov, and Hyunjin Ju (2021)**

This paper provides an excellent overview of the shear design equations. Their elaborate explanation of information regarding the "Detailed Method" and their explanation of the $\boldsymbol{V_{ci}}$ and $\boldsymbol{V_{cw}}$ equations were extremely helpful in understanding the current methods of shear design within prestressed concrete. The authors filtered through an existing large shear testing database and removed any members that were unrealistic and created new recommendations based on their findings. Their suggested equations are listed below along with the current equations for reference.

$$V_{ci}\ = 0.6\lambda\sqrt{f_c'}b_w d_p + V_d + \frac{V_i M_{cre}}{M_{max}} \qquad \text{ACI 18-19 22.5.6.3.1}$$

$$V_{ci}\ = 0.6\lambda K\sqrt{f_c'}b_w d_p + \frac{V_u M_{cr}}{M_u} \qquad \text{Proposed Equation}$$

$$V_{cw} = \left(3.5\lambda\sqrt{f_c'} + 0.3\ f_{pc}\right)b_w d_p + V_p \qquad \text{ACI 18-19 22.5.6.3.2}$$

$$V_{cw} = \left(2\lambda K\sqrt{f_c'} + 12\ \sqrt{f_{pc}}\right)b_w d_p + V_p \qquad \text{Proposed Equation.}$$

Where:

$$K = 4\rho_{wt}^{1/3} \leq 1 \qquad \text{Eq 2.4C}$$

$$\rho_{wt} = A_s/(b_w d) + A_{ps}/(b_w d) \qquad \text{Eq 2.4D}$$

$$M_{cre} = \left(6\lambda\sqrt{f_c'} + f_{pe} - f_d\right)I/y \quad \text{Eq 2.4E}$$

$$M_{cr} = \left(7.5\lambda\sqrt{f_c'} + f_{pe}\right)I/y \quad \text{Eq 2.4F}$$

The changes to the equations reflect the various trends they observed in the data. The authors propose removing the V_d term from the V_{ci} equation because its influence is marginal. This allows M_{cre} to become independent of the dead load effect, eliminating the f_d from the equation. Based on the authors experiments, these slight changes, the removal of V_d can cause up to a 10% difference on the unconservative side of the proposed equation when compared to the ACI equation. After making this slight change, the authors realized that as their reinforcement ratio (ρ_{wt}) changed within their new equation, their capacity estimates become more conservative. To adjust the equation to reflect the capacity more accurately, the constant K was derived using the ρ_{wt}.

These changes were enough to warrant the authors approval for the V_{ci} equation, but additional considerations were needed for the V_{cw} equation. After reviewing research done by Saqan and Frosch, the authors concluded that the reinforcement ratio should also be considered for the V_{cw} equation (Saqan, Frosh 2009). In addition, the authors discovered that the slope of the capacity line would be more accurately followed by using $\sqrt{f_{pc}}$ instead of just f_{pc}. After making this slight change, and when considering the addition of the reinforcement ratio (ρ_{wt}), the constants were adjusted to better fit the line, and that is why the original 3.5 and 0.3 changed to a 2 and 12 in the new equation.

The authors go on to verify the legitimacy of their proposed equations and conclude with the request to have their equations considered within the upcoming code cycle. At this time, the impacts of these proposed equations and discoveries within this project have not been realized, but it does prove to be a major indicator that while current shear equations work, there is reason to believe that they need modification to adapt to recent changes in material quality and recent research.

2.5 Summary

The code equations regarding shear for prestressed members have evolved since their first inclusion in the 318 code. In the current code, 318-19, designers have two options for prestressed concrete in shear: the simplified method or the detailed method. The vast majority of designers use the detailed method since it best follows the predicted behavior with inclusion of two types of shear cracking (web and inclined shear). This method is relatively straight forward for pretensioned determinate members. For post-tensioned members, the vertical prestressing term (V_p) is continuously changing due to the parabolic tendon shape. These members are also often continuous multi-span beams making the calculations more complex without much gain in economy since shear reinforcement is typically used as with other cast-in-place structures. The new shear equations for non-prestressed concrete show promise as a simplified option for post-tensioned members with the addition of a term in the same form of the axial load term. This research will evaluate coefficients for the additional term and compare the results to the shear reinforcement requirements of the detailed method. The proposed summary is listed below. The new ACI 320 Post-Tensioned Concrete Code to be published in 2025 is the most likely place for a new equation of this type.

$$V_c = (2\lambda\sqrt{f_c'} + \frac{N_u}{6A_g} + \frac{P}{mA_g})b_w d \qquad \text{New Proposed Equation}$$

Where:

N_u= Axial Force

P = Prestressing Force

$m =$ Constant used to calibrate proposed equation in parametric study

$d =$ Distance to prestressing strand from bottom of member

Chapter 3: Work Plan

3.1 Introduction

To verify that our proposed shear equation would be a conservative alternative to the detailed shear design method, an Excel file was developed to calibrate our new model and provide a meaningful outcome within a parametric study. The most directly comparable results the models produced was a percent and total change in stirrups needed between the detailed method and our proposed equation, as well as the V_c along the length of the beam. If engineers know the percent and total change in the number of rebars required in each method, then the decision on whether to use the new method given a trade off in design time vs additional stirrups is easier to make. The rest of this section discusses the design process, other considerations in the data analysis, an in-depth discussion of two examples that were analyzed for this parametric study, and a brief summary of the other three examples used the development of this thesis.

3.2 Parametric Study

An Excel file was created to determine a member's response to loading, and a current shear design solution given the members geometry, loading conditions, and length of span. After following the design process as discussed in section 2.3.2**:** Current Shear Design Procedure for Prestressed Members (Detailed Method), a workable shear design was created for each member that functioned as a control. Next, an identical shear design was followed, but our proposed equation was used to determine concrete shear strength rather than the detailed method. This yielded our test data. The equations for determining concrete contribution for the detailed and new method are restated below.

$$V_c = minimum\ (V_{ci}\ , V_{cw}) \qquad \text{Detailed Method}$$

$$V_{ci} = 0.6\lambda\sqrt{f_c'}b_w d_p + V_d + \frac{V_i M_{cre}}{M_{max}} \qquad \text{ACI 18-19 22.5.6.3.1}$$

$$V_{cw} = \left(3.5\lambda\sqrt{f_c'} + 0.3\ f_{pc}\right)b_w d_p + V_p \qquad \text{ACI 18-19 22.5.6.3.2}$$

$$V_c = (2\lambda\sqrt{f_c'} + \frac{N_u}{6A_g} + \frac{P}{mA_g})b_w d \qquad \text{Proposed Equation}$$

The proposed equation is much more simplistic than the Detailed Method. Notice how the proposed equation acts independently from the loading of the structure and relies on fewer terms in the equation. Additionally, the N_u term in the proposed equation goes to zero when analyzing beams with no additional axial load (as would be typical for PS members). The detailed method provided a baseline to which the proposed equation could be tested, calibrated, and effectively compared.

The calibration of the proposed equation focuses on the constant m. An increase in the m term of the proposed equation results in a decrease of V_c and a decrease in the m term results in an increase of V_c if all other variables are held constant. The value of m at which the new equation is always conservative compared to the detailed method varies depending on loading condition, geometry, and the support structure of the concrete member; however, the goal of the calibration was to find the smallest reasonable m value that is conservative in typical PT beam configurations.

One limiting factor when calibrating the proposed equation is to ensure only reasonable sections are analyzed. A reasonable section for this parametric study is considered one that passes the initial transfer checks and has a realistic strand pattern. The examples analyzed for this thesis all passed the transfer checks and have realistic strand patterns. The beam dimensions were taken from designs provided by design consultants in the PT industry.

Two different types of members were tested for the calibration of this model: simply supported with an overhang, and continuous beams. The overhang model investigates the reversal of moments and tendon profile while still being a determinant member. Continuous beams are commonly designed as PT members that also have reversing moments in the member. In sections 3.3 and 3.4 an example of each will be provided to illustrate what members are being analyzed for this thesis. Results from these examples can be found in section 4.2 and 4.3.

3.3 Overhang Beam Example

A simply supported member with an overhang, as shown in figure 3.3A, is a member with two supports: one support is at the end of the beam and the other support is near, but not at the other end of the beam, causing some portion of the beam to overhang and have a reversal of moments. The beam shown in Figure 3.3A was one of the examples used to create our model. The cross-section information for this beam is listed in Figure 3.3B. After following the steps outlined in section 2.3.2, the following V_c graph in Figure 3.3C is the result from the detailed method approach. The initial conditions and loading information for this example are as follows**:** 12 Prestressing Strands; f_c' = 5 ksi; dead load (DL) (self-weight included) = 2 klf; live load (LL) = 1.5 klf

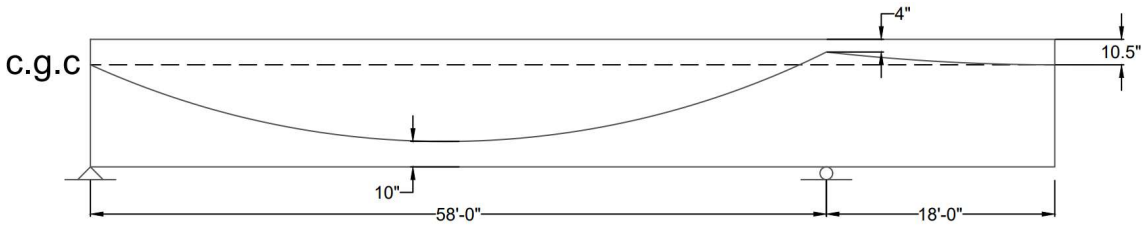

Figure 3.3A: Overhang Beam Tendon Profile

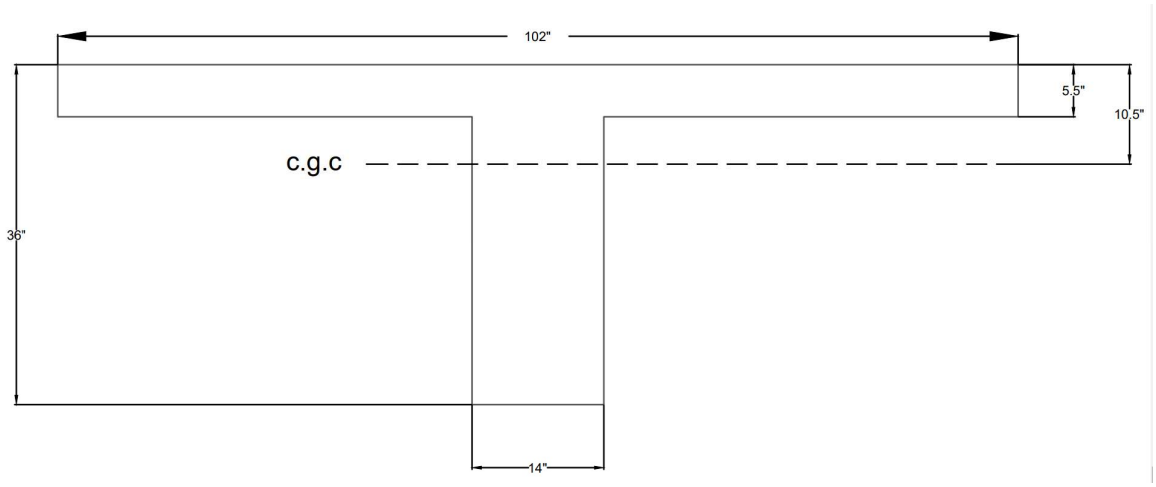

Figure 3.3B: Section View

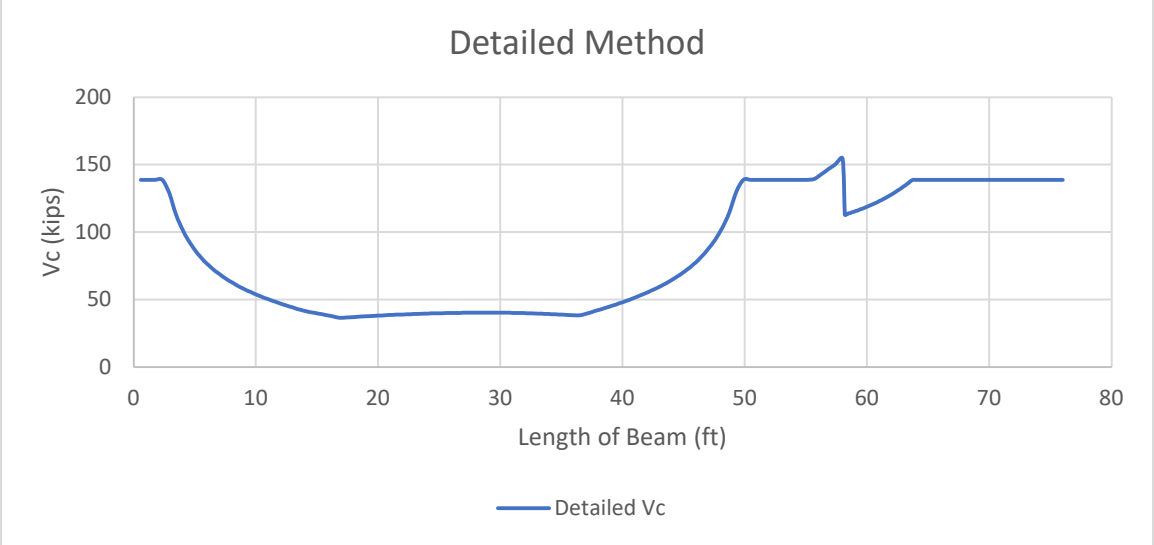

Figure 3.3C: Detailed Method Concrete Shear Strength (Overhang Beam)

With the detailed method completed, the parametric study as explained in Section 3.2 could begin. The results of this example can be found in Section 4.2.

3.4 Continuous Beam Example

A continuous structure, as shown in figure 3.4A, is a member with more than one span: one support is at the end of the beam and the others are spaced out along the length of the beam. The beam shown in Figure 3.4A was one of the examples used to create our model. The cross section for this beam is listed in Figure 3.4B. After following the steps outlined in section 2.3.2, the following V_c graph in Figure 3.4C is the result from the detailed method approach. The initial conditions and loading information for this member are as follows**:** Unbonded Tendons; 10 Prestressing Strands; f_c' = 4 ksi; DL = 2.2 klf; LL = 1.2 klf

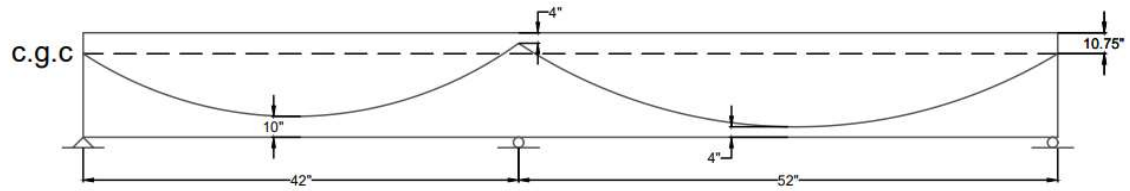

Figure 3.4A: Continuous Beam Tendon Profile

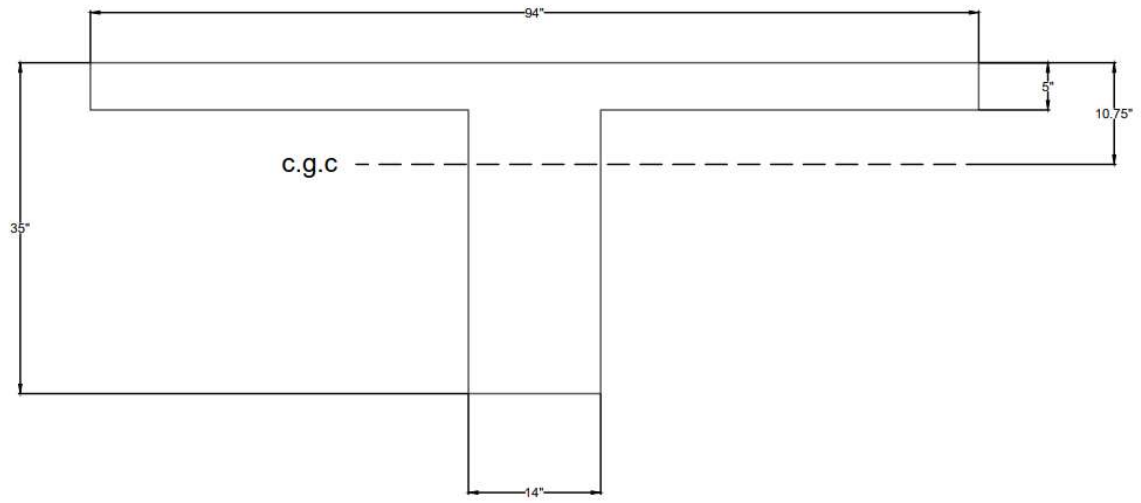

Figure 3.4B: Section View and Loading Condition (Bondy 2019)

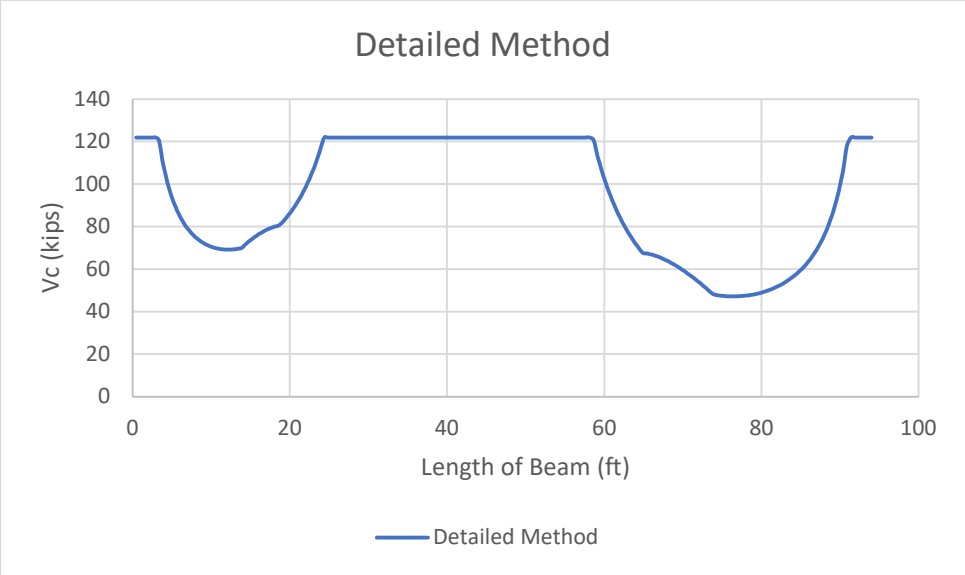

Figure 3.4C: Detailed Method Concrete Shear Strength (Continuous Beam)

With the detailed method completed, the parametric study as explained in Section 3.2 could begin. The results of this example can be found in Section 4.3.

Chapter 4: Results and Discussion

4.1 Introduction

A total of five examples (two overhang and three continuous beams) were analyzed for this thesis. These five examples were subjected to hypothetical changes in the number of prestressing strands in the member while still being a reasonable member (logical number of strands and passes transfer checks). This section contains the detailed results of the two example problems stated sections 3.3 and 3.4, a summary of data resulting from the changing of the m term and number of strands in the two example problems, and a summary of the data resulting from the other three examples.

4.2 Overhang Example Results

With the detailed method determined, a calibration of our new equation could take place. The m term in our new equation was started at 1 and was increased by 0.5 until a value was found where the new method was always conservative compared to the detailed method. The lowest m value for this problem that ended up being conservative at all points was 7.0. To show how changing the m value affects the estimated V_c, Figure 4.2A shows the detailed method compared to a m = 2.0 and Figure 4.2B shows the detailed method compared to m = 7.0. The m = 2.0 model follows the general shape of the detailed model most accurately but doesn't provide a conservative solution at midspan. In order to have a fully conservative solution, the m value had to be raised to 7, resulting in overly conservation solutions near the support (where V_{cw} would typically control in the detailed method).

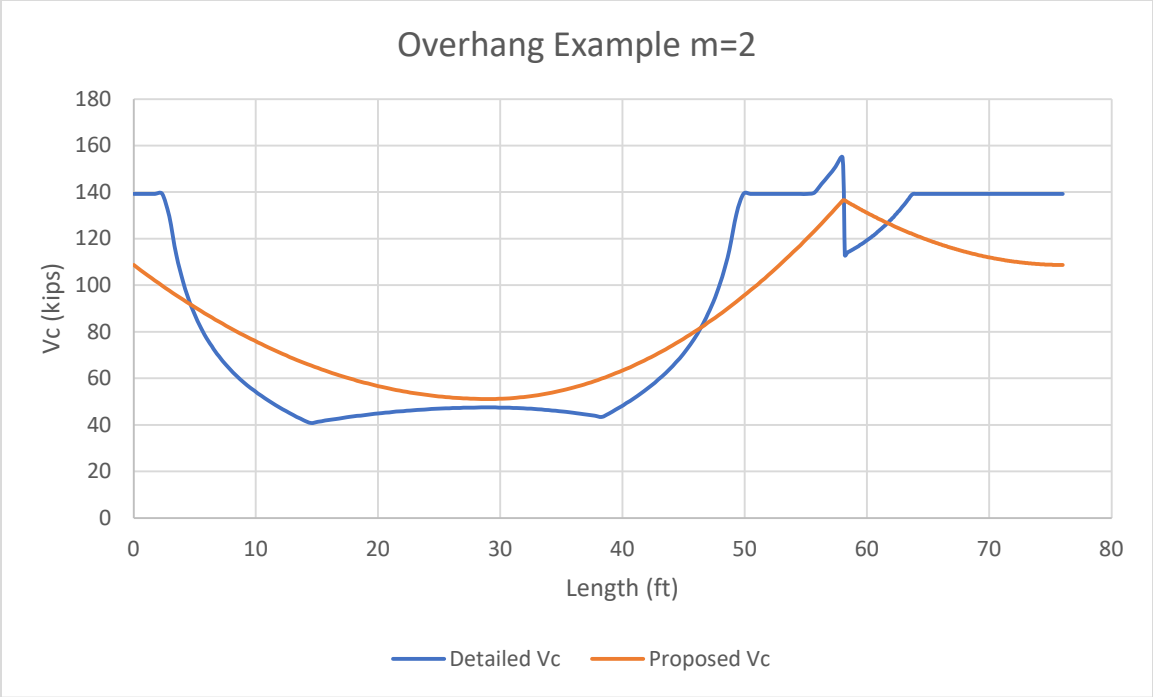

Figure 4.2A: Detailed Method vs m=2.0

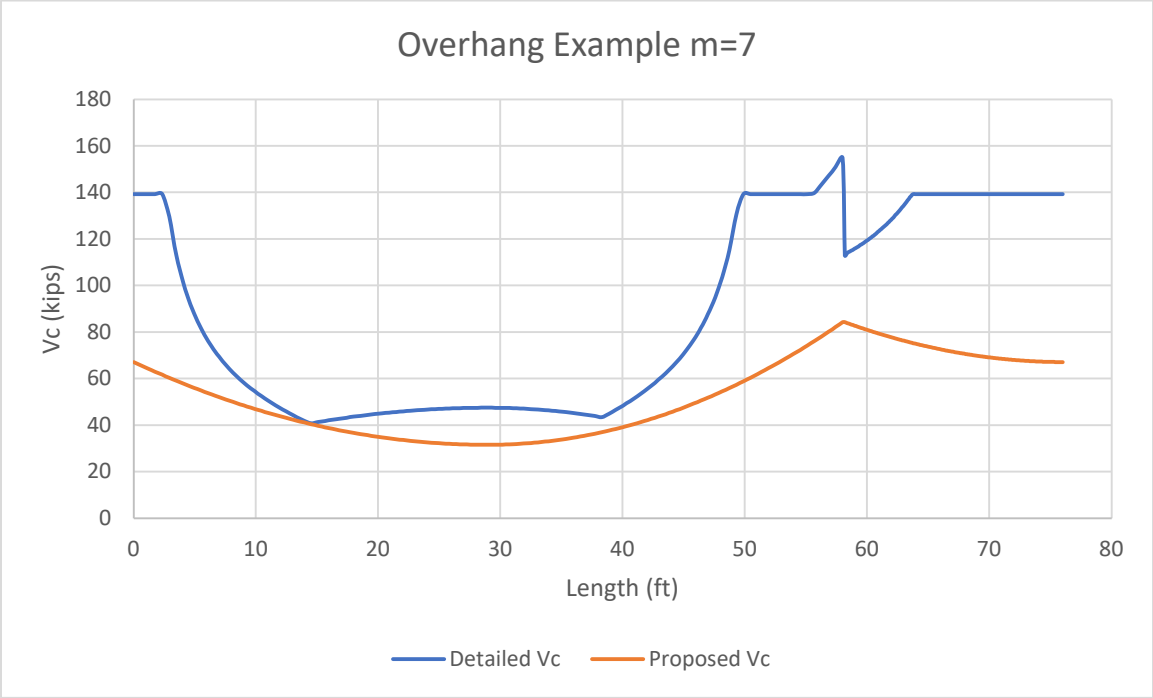

Figure 4.2B: Detailed Method vs m=7.0

After a value for m is determined, the exact same shear design methodology used for the detailed method is applied to the proposed V_c equation. With the total number of rebar determined from both methods, the difference between the two methods is clear to see. Table 4.2C below illustrates the results when comparing the Detailed Method and the proposed V_c equation when the m value is equal to 7.

Method	Number of #3 Rebar	% Difference
Detailed	45	0
Proposed	62	38%

Table 4.2C: Detailed Vs Proposed Equation Rebar Comparison

With the comparison between the two methods now complete, the minimum m value was recorded along with the difference in total rebar used, and the percent difference. With an overhang Excel sheet now complete and able to be easily modified for new cross sections and varying number of prestressing strands, the focus shifted to completing the same analysis, but for a continuous structure.

4.3 Continuous Example Results

With the detailed method determined, a calibration of our new equation could take place. The m term in our new equation was started at 1 and was increased by 0.5 until a value was found where the new method was always conservative compared to the detailed method. The m value for this problem that ended up being conservative at all points was 2.5. To show how changing the m value affects the estimated V_c, Figure 4.3A shows the detailed method compared to a m = 1.0 and Figure 4.3B shows the detailed method compared to m = 2.5. Again, the areas near supports are the most conservative, but the

general curve fit for the continuous beam matches the detailed method solution well away from the supports.

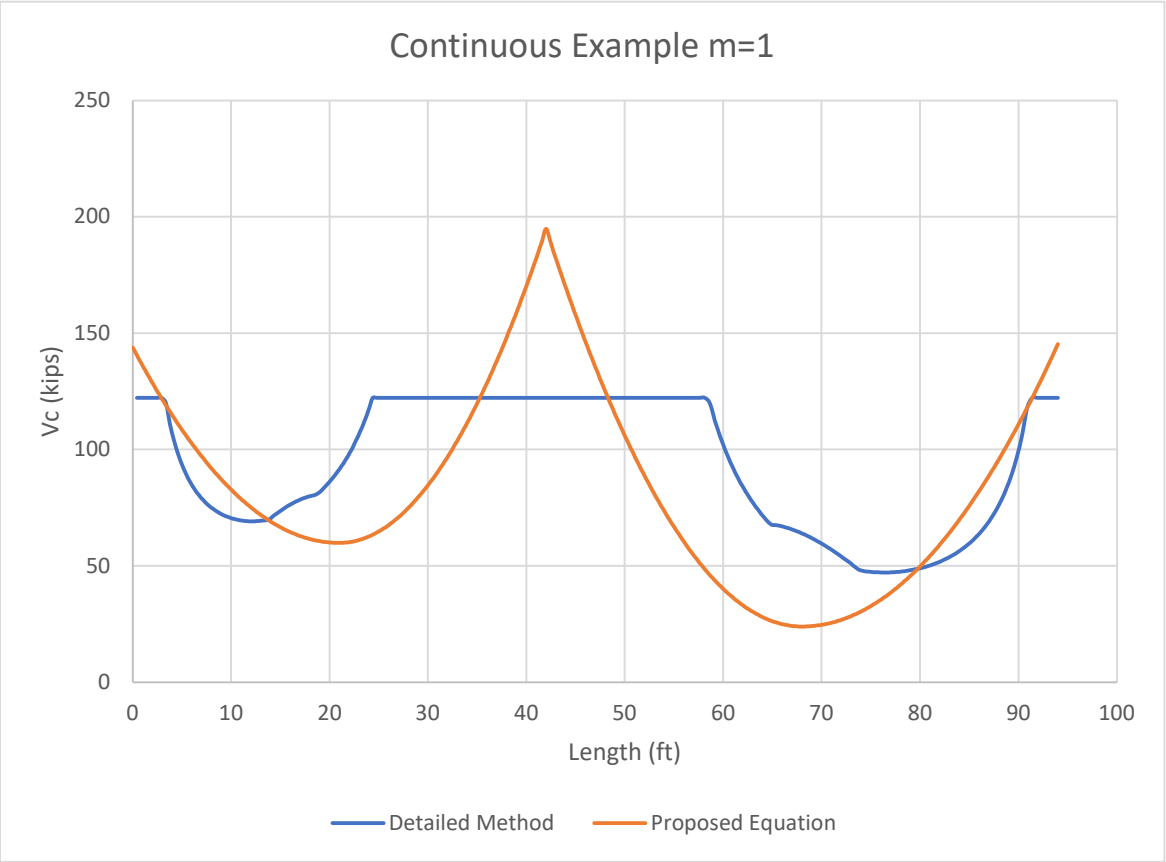

Figure 4.3A: Detailed Method vs m=1.0

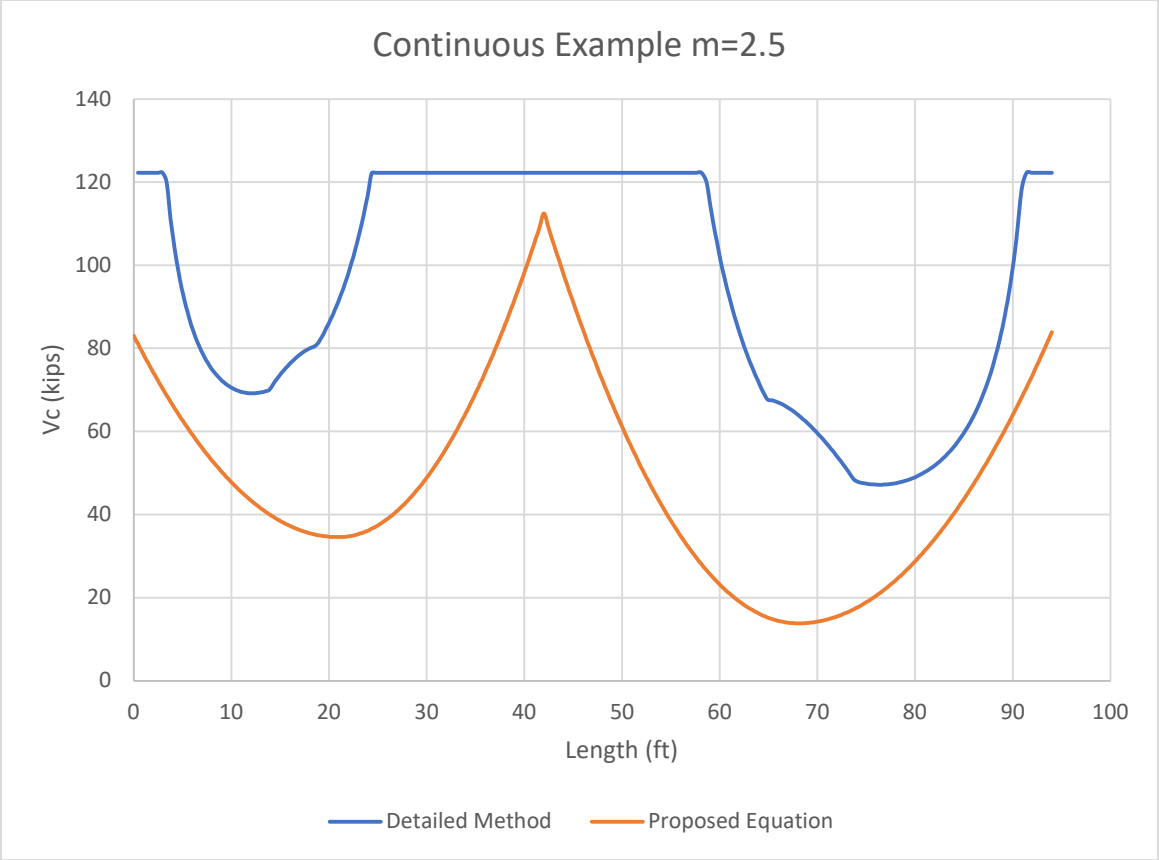

Figure 4.3B: Detailed Method vs m=2.5

After a value for m is determined, the exact same shear design methodology used for the detailed method is applied to the proposed V_c equation. With the total number of rebar determined from both methods, the difference between the two methods is clear to see. Table 4.3C below illustrates the results when comparing the detailed method and the proposed V_c equation when the m value is equal to 2.5.

Method	Number of #3 Rebar	% Difference
Detailed	42	0
Proposed	80	90

Table 4.3C: Detailed Vs Proposed Equation Rebar Comparison

With the comparison between the two methods now complete, the minimum m value was recorded along with the difference in total rebar used, and the percent difference. With an Excel sheet now complete for continuous structures, the rest of the analysis could commence.

4.4 Overhang Example Calibration with Different Number of Strands

After the initial condition was calibrated, the number of strands were changed to see how changing the prestressing force affected the difference between the detailed method and the proposed equation. Changing the number of prestressing strands affect the $\frac{P}{mA_g}$ term in the proposed equation. This results in the changing of the value of m for which the proposed equation is targeted to always be conservative when compared to the detailed method. A table summarizing multiple strand variations, as well as the resulting change in number and percent of rebar in the member when comparing the two equations for the overhang example is listed in table 4.4A below. Only m values that resulted in the proposed equation being conservative along the entire length of the beam were reported and all reported number of strands options are realistic sections.

Overhang Example																				
P/A			217 (8 strands)				271 (10 strands)				326 (12 strands)				480 (14 strands)				435(16 strands)	
m value	Detailed	Proposed	Rebar Diff	% Diff	Detailed	Proposed	Rebar Diff	% Diff	Detailed	Proposed	Rebar Diff	% Diff	Detailed	Proposed	Rebar Diff	% Diff	Detailed	Proposed	Rebar Diff	% Diff
4	49	60	11	22																
4.5	49	62	13	27																
5	49	63	14	29	47	60	13	28												
5.5	49	64	15	31	47	61	14	30												
6	49	65	16	33	47	62	15	32												
6.5	49	66	17	35	47	63	16	34												
7	49	66	17	35	47	64	17	36	45	62	17	38	42	60	18	43	39	59	20	51
7.5	49	67	18	37	47	65	18	38	45	63	18	40	42	61	19	45	39	60	21	54
8	49	68	19	39	47	66	19	40	45	64	19	42	42	62	20	48	39	60	21	54
8.5	49	68	19	39	47	66	19	40	45	64	19	42	42	63	21	50	39	61	22	56
9	49	69	20	41	47	67	20	43	45	65	20	44	42	63	21	50	39	62	23	60

Table 4.4A: Overhang Example Varying Number of Prestressing Strands

As shown in table 4.4A, the conservative m value increases as the prestressing force increases. This confirms the hypothesis that the $\frac{P}{mA_g}$ term which relates to total stress from PS in the proposed equation is the key variable and the value of m can be used to shift the equation to be conservative compared to the detailed method. Also, the effect of increasing the m value by 0.5 decreases as the m value gets higher.

4.5 Continuous Example Calibration with Different Number of Strands

The same variation that was applied to the overhang example, as explained in previous section was applied to the continuous example as well. A table summarizing multiple strand variations, as well as the resulting change in number and percent of rebar in the member when comparing the two equations for the continuous example is listed in table 4.5A below. Only m values that resulted in the proposed equation being conservative along the entire length of the beam were reported and all reported number of strands options are realistic sections.

Continuous Example																				
P/A	241.4 (8 strands)				301.7 (10 strands)				362 (12 strands)				422 (14 strands)				483 (16 strands)			
m value	Detailed	Proposed	Rebar Diff	% Diff	Detailed	Proposed	Rebar Diff	% Diff	Detailed	Proposed	Rebar Diff	% Diff	Detailed	Proposed	Rebar Diff	% Diff	Detailed	Proposed	Rebar Diff	% Diff
2	43	80	37	86	42	74	32	76	41	67	26	63								
2.5	43	84	41	95	42	80	38	90	41	75	34	83	41	69	28	68				
3	43	87	44	102	42	83	41	98	41	80	39	95	41	75	34	85	40	71	31	78
3.5	43	89	46	107	42	86	44	105	41	83	42	102	41	80	39	95	40	76	36	90
4	43	91	48	112	42	88	46	110	41	85	44	107	41	82	41	100	40	80	40	100
4.5	43	93	50	116	42	90	48	114	41	87	46	112	41	84	43	105	40	82	42	105
5	43	95	52	121	42	91	49	117	41	89	48	117	41	86	45	110	40	84	44	110
5.5	43	96	53	123	42	93	51	121	41	90	49	120	41	88	47	115	40	85	45	123
6	43	97	54	126	42	94	52	124	41	91	50	122	41	89	48	117	40	87	47	118
6.5	43	98	55	128	42	95	53	126	41	93	52	137	41	90	49	120	40	88	48	120
7	43	98	55	128	42	96	54	129	41	94	53	129	41	91	50	122	40	89	49	123
7.5	43	99	56	130	42	97	55	131	41	95	54	132	41	93	52	127	40	90	50	125
8	43	100	57	133	42	97	55	131	41	95	54	132	41	93	52	127	40	91	51	128
8.5	43	100	57	133	42	98	56	133	41	96	55	134	41	94	53	129	40	92	52	130
9	43	101	58	135	42	99	57	136	41	97	56	137	41	95	54	132	40	93	53	133

Table 4.5A: Continuous Example Varying Number of Prestressing Strands

The continuous beam has less variance that the overhang beam with a peak m value of 4 for the given scenario.

4.6 Additional Examples

This section contains the other three examples that were used for the development of this thesis. The three examples contain an additional overhang member, two-span continuous member, and a three-span continuous member. These members are either overhang or continuous structures with slight variations to the examples. Each example is detailed in the following sections. The continuous beams in this section were taken from actual building plans.

4.6.1 Second Overhang Example

A second overhang member was analyzed to compare to the example given in section 3.3. This second overhang member is relatively similar to the first; however, it has a slightly lower load, wider flange, smaller compressive concrete strength, and more prestressing strands. The cross section, strand profile for the and results are in the figures below. The initial conditions and loading information for this example are as follows**:** 14 Prestressing Strands; f_c' = 4 ksi; DL = 2.2 klf; LL = 1 klf

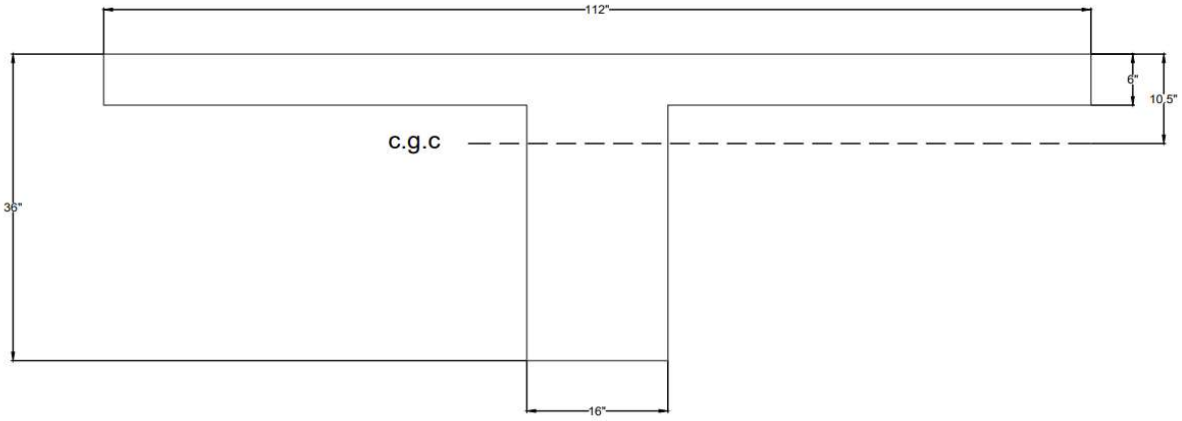

Figure 4.6.1A: Cross Section of Second Overhang Example

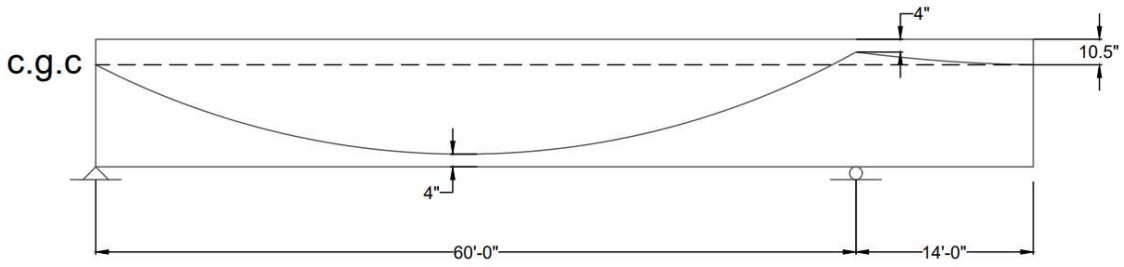

Figure 4.6.1B: Tendon Profile of Second Overhang Example

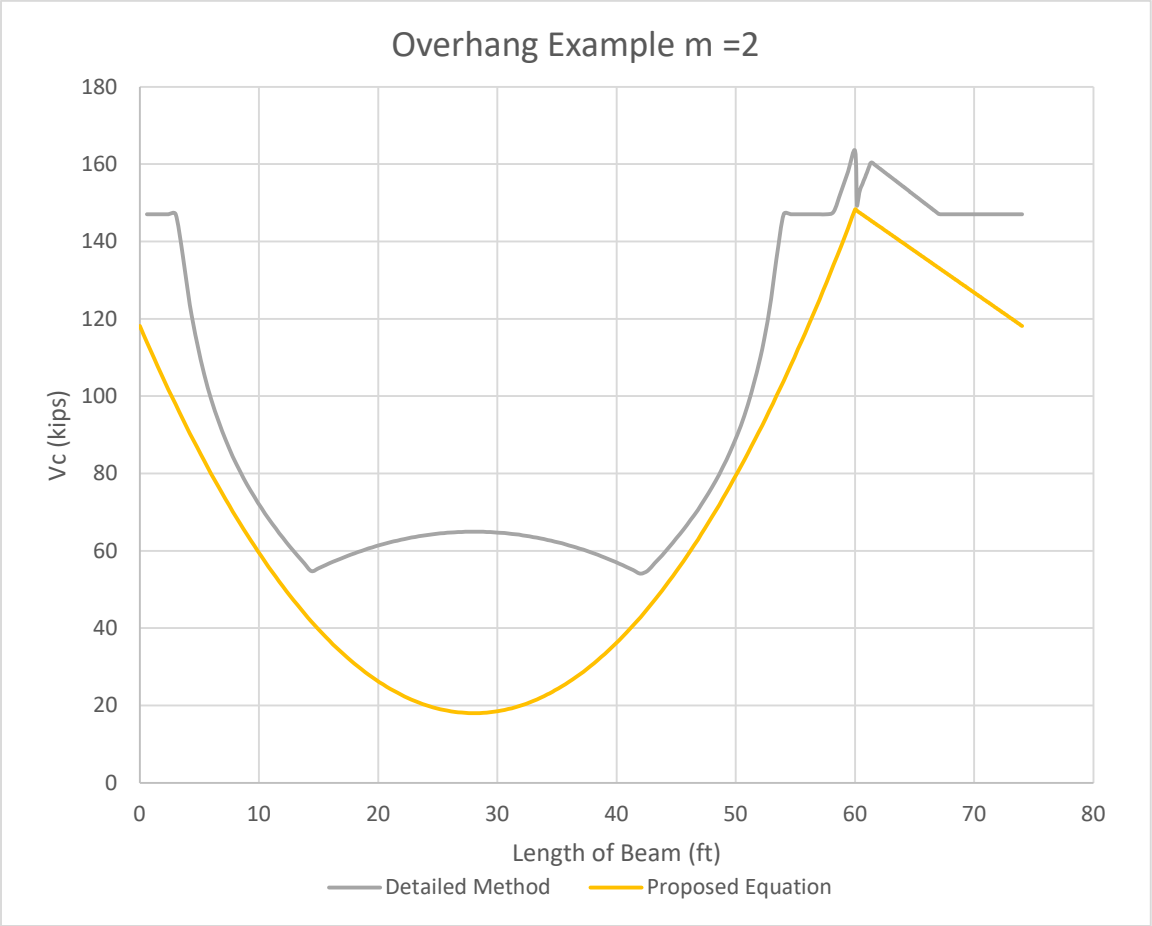

Figure 4.6.1C: Results of Second Overhang Example

Method	Number of #3 Rebar	% Difference
Detailed	27	0
Proposed	43	59%

Table 4.6.1D: Detailed Vs Proposed Equation Rebar Comparison

Second Overhang Example																				
P/A			280 (12 strands)				326 (14 strands)				373 (16strands)				420(18 strands)				466(20strands)	
m value	Detailed	Proposed	Rebar Diff	% Diff	Detailed	Proposed	Rebar Diff	% Diff	Detailed	Proposed	Rebar Diff	% Diff	Detailed	Proposed	Rebar Diff	% Diff	Detailed	Proposed	Rebar Diff	% Diff
2	30	48	18	6	27	43	16	59	24	38	14	58	22	34	12	55	21	30	9	43
2.5	30	52	22	73	27	49	22	71	24	46	22	92	22	42	20	91	21	38	17	81
3	30	54	24	80	27	52	25	96	24	50	26	108	22	48	26	118	21	45	24	144
3.5	30	56	26	87	27	54	27	100	24	53	29	121	22	51	29	131	21	49	28	133
4	30	57	27	90	27	56	29	107	24	54	30	125	22	53	31	141	21	51	30	143
4.5	30	58	28	93	27	56	29	104	24	56	32	133	22	54	32	145	21	53	32	152
5	30	59	29	97	27	58	31	115	24	57	33	138	22	56	34	155	21	54	33	157
5.5	30	60	30	100	27	59	32	119	24	58	34	142	22	57	35	159	21	56	35	167
6	30	60	30	100	27	59	32	119	24	58	34	142	22	57	35	159	21	56	35	167
6.5	30	60	30	100	27	60	33	122	24	59	35	146	22	58	36	164	21	57	36	171
7	30	61	31	103	27	60	33	122	24	59	35	146	22	59	37	168	21	58	37	176
7.5	30	61	31	103	27	60	33	122	24	60	36	150	22	59	37	168	21	58	37	176
8	30	61	31	103	27	61	34	126	24	60	36	150	22	59	37	168	21	59	38	181
8.5	30	62	32	107	27	61	34	126	24	60	36	150	22	60	38	173	21	59	38	181
9	30	62	32	107	27	61	34	126	24	61	37	154	22	60	38	173	21	59	38	181

Table 4.6.1E: Varying Strand Numbers of Second Overhang Example

When compared to the first overhang example, the second example has a m value of 2 which is significantly lower than the m value of 7 in the first example; however, the percent difference between the detailed and proposed equation is not much higher in the second example (59%) than in the first (38%). The large difference between the two overhang examples is concerning when trying to determine a conservative m value for the proposed equation.

4.6.2 Second Continuous Example

A second continuous member was analyzed to compare to the example given in section 3.4. This second continuous member has longer spans than the first example with fewer prestressing strands and smaller loads, but the concrete strength is more in the second example. The cross section, strand profile for the and results are in the figures below. The

initial conditions and loading information for this example are as follows**:** 9 Prestressing Strands; f_c' = 5 ksi; DL = 1.7 klf; LL = 800 plf

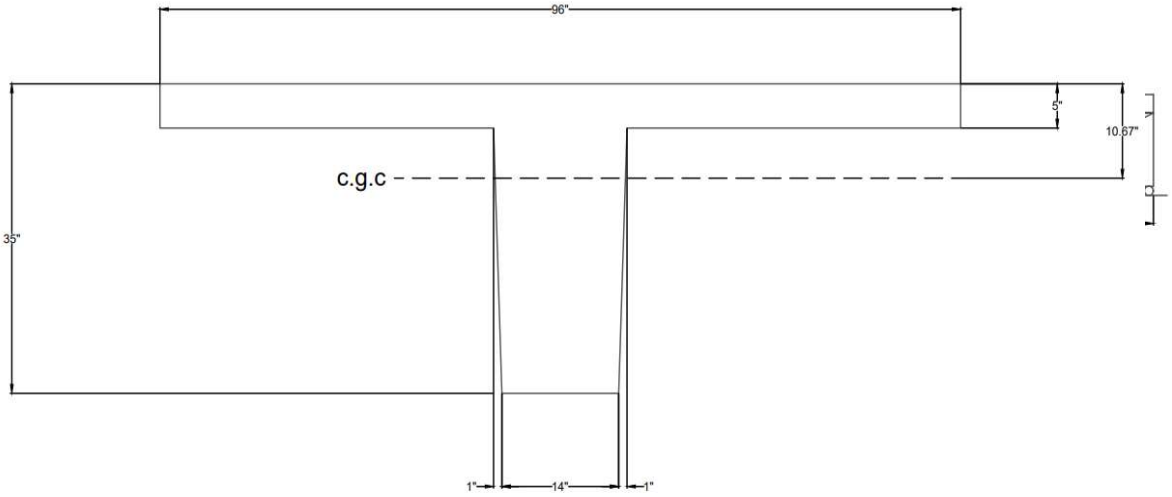

Figure 4.6.2A: Cross Section of Second Continuous Example

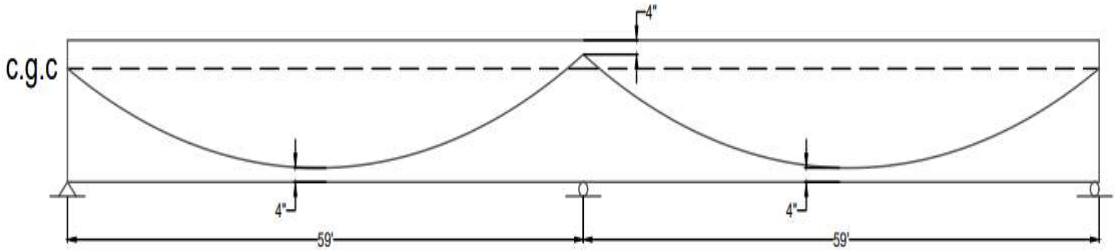

Figure 4.6.2B: Tendon Profile of Second Continuous Example

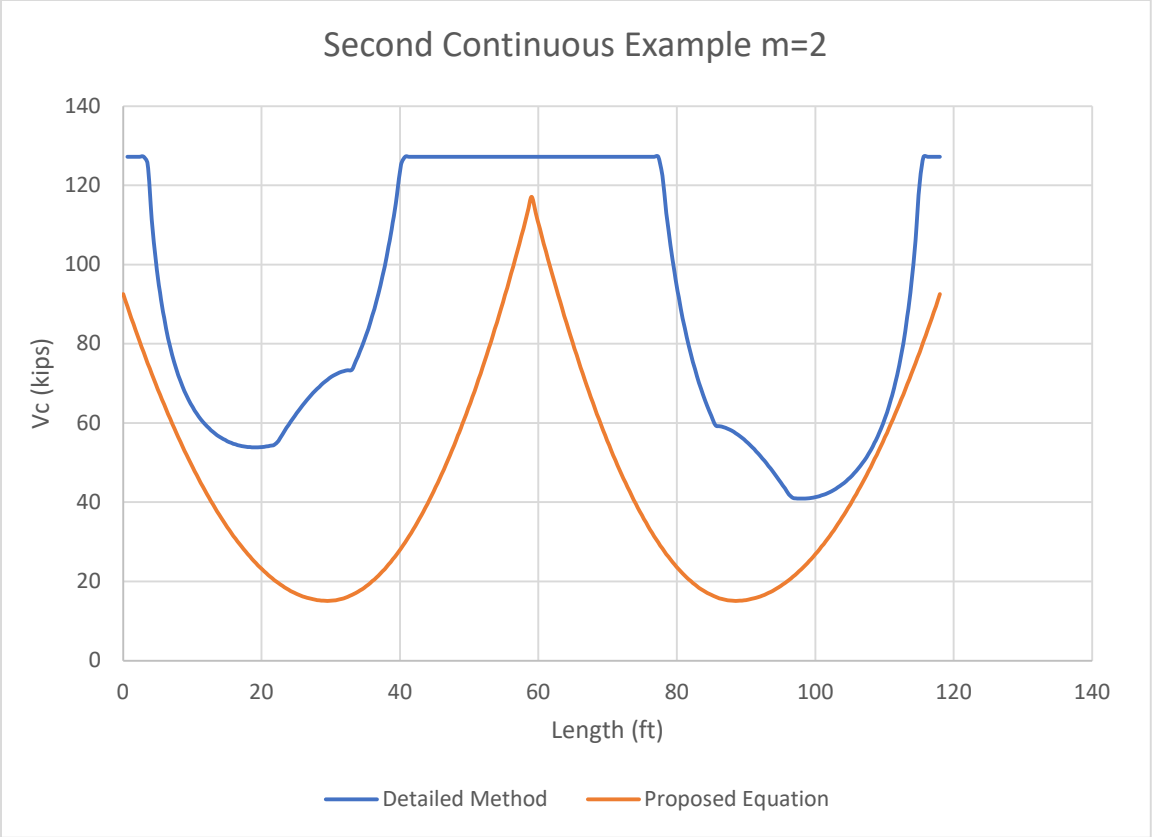

Figure: 4.6.2C: Results of Second Continuous Example

Method	Number of #3 Rebar	% Difference
Detailed	42	0
Proposed	72	71

Table 4.6.2D: Detailed Vs Proposed Equation Rebar Comparison

Second Continuous Example																				
P/A	86 (3 strands)				171 (6 strands)				257 (9 strands)				343 (12 strands)				483 (15 strands)			
m value	Detailed	Proposed	Rebar Diff	% Diff	Detailed	Proposed	Rebar Diff	% Diff	Detailed	Proposed	Rebar Diff	% Diff	Detailed	Proposed	Rebar Diff	% Diff	Detailed	Proposed	Rebar Diff	% Diff
2	45	92	47	104	43	79	36	84	42	72	30	70	40	68	28	70	40	62	22	55
2.5	45	94	49	109	43	84	41	95	42	74	32	76	40	72	32	80	40	68	28	70
3	45	96	51	113	43	87	44	102	42	79	37	88	40	74	34	85	40	71	31	78
3.5	45	97	52	116	43	90	47	109	42	83	41	98	40	75	35	88	40	73	33	83
4	45	98	53	118	43	92	49	114	42	85	43	102	40	79	39	98	40	74	34	85
4.5	45	98	53	118	43	93	50	116	42	87	45	107	40	82	42	105	40	76	36	90
5	45	99	54	120	43	94	51	119	42	89	47	112	40	84	44	110	40	79	39	98
5.5	45	99	54	120	43	95	52	121	42	91	49	117	40	86	46	115	40	81	41	103
6	45	100	55	122	43	96	53	123	42	92	50	119	40	87	47	118	40	83	43	108
6.5	45	100	55	122	43	96	53	123	42	93	51	121	40	89	49	123	40	85	45	113
7	45	100	55	122	43	97	54	126	42	93	51	121	40	90	50	125	40	86	46	115
7.5	45	100	55	122	43	97	54	126	42	94	52	124	40	91	51	128	40	87	47	118
8	45	101	56	124	43	98	55	128	42	95	53	126	40	92	52	130	40	89	49	123
8.5	45	101	56	124	43	98	55	128	42	95	53	126	40	92	52	130	40	90	50	125
9	45	101	56	124	43	98	55	128	42	96	54	129	40	93	53	133	40	90	50	125

Table 4.6.2E: Varying Strand Numbers of Second Continuous Example

When compared to the first continuous example, the second example has a m value of 2 which is slightly less than the m value of 2.5 in the first example; however, the percent difference between the detailed and proposed equation is not as close between the second example (71%) and the first (90%). The difference between the two continuous examples is enough to warrant more data points needing to be tested, but close enough that there seems to be hope that continuous members will not have the large amount of variation between m values that the overhang examples displayed in earlier tests.

4.6.3 Third Continuous Example

A third continuous member was analyzed to compare to the example given in section 3.4. This third continuous member has the exact same loading, cross section, number of strands, and span lengths as the example in section 4.6.2. The only difference between this example and the one in section 4.6.2 is that this example has an additional middle span. This example provides a valuable variation and illustrates trends that would likely continue if more middle spans were added for longer structures. The cross section and strand profile for the and results are in the figures below. The initial conditions and loading information for this example are as follows**:** 9 Prestressing Strands; f_c' = 5 ksi; DL = 1.7 klf; LL = 800 plf

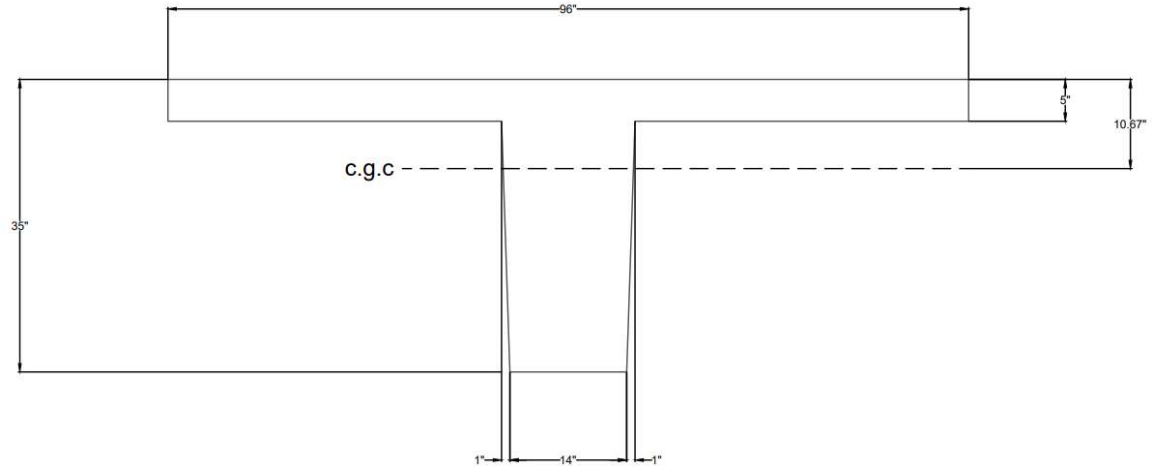

Figure 4.6.3A: Cross Section of Third Continuous Example

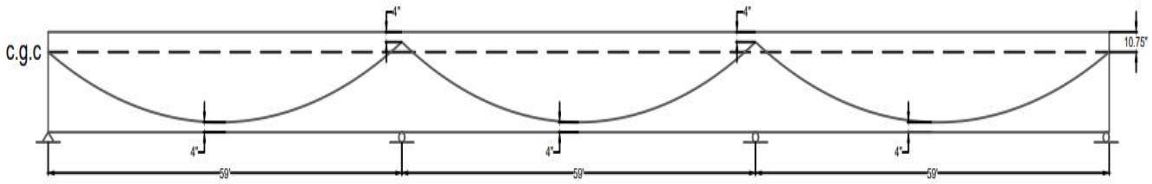

Figure 4.6.3B: Tendon Profile of Third Continuous Example

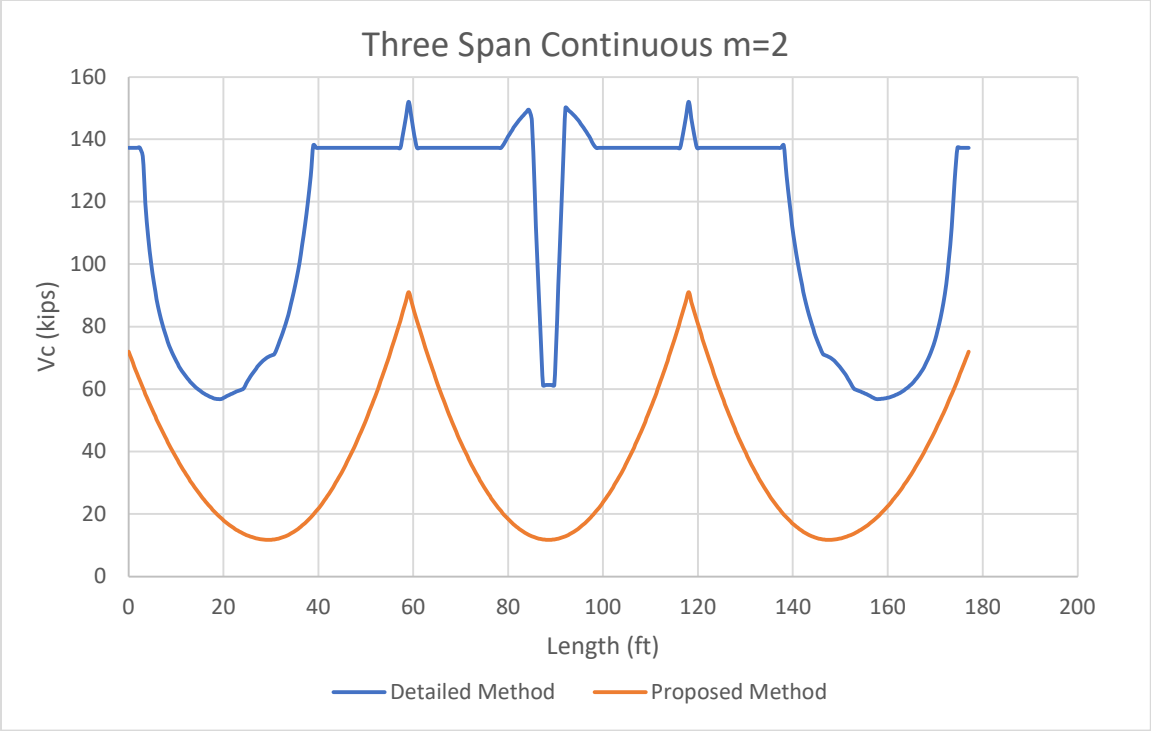

Figure: 4.6.3C: Results of Third Continuous Example

Method	Number of #3 Rebar	% Difference
Detailed	25	0
Proposed	50	100

Table 4.6.3D: Detailed Vs Proposed Equation Rebar Comparison

Third Continuous Example																				
P/A	86 (3 strands)				171 (6 strands)				257 (9 strands)				343 (12 strands)				483 (15 strands)			
m value	Detailed	Proposed	Rebar Diff	% Diff	Detailed	Proposed	Rebar Diff	% Diff	Detailed	Proposed	Rebar Diff	% Diff	Detailed	Proposed	Rebar Diff	% Diff	Detailed	Proposed	Rebar Diff	% Diff
2	28	63	35	125	27	55	28	104	25	50	25	100	23	47	24	104	19	45	26	137
2.5	28	66	38	136	27	57	30	111	25	53	28	112	23	49	26	113	19	47	28	147
3	28	68	40	143	27	60	33	122	25	55	30	120	23	52	29	126	19	49	30	158
3.5	28	69	41	146	27	62	35	130	25	56	31	124	23	53	30	130	19	51	32	168
4	28	70	42	150	27	63	36	133	25	58	33	132	23	55	32	139	19	52	33	174
4.5	28	71	43	154	27	65	38	141	25	60	35	140	23	56	33	144	19	54	35	184
5	28	71	43	154	27	66	39	144	25	61	36	144	23	57	34	148	19	55	36	190
5.5	28	72	44	157	27	67	40	148	25	62	37	148	23	59	36	157	19	56	37	195
6	28	72	44	157	27	68	41	152	25	63	38	152	23	60	37	161	19	57	38	200
6.5	28	73	45	161	27	68	41	152	25	64	39	156	23	61	38	165	19	58	39	205
7	28	73	45	161	27	69	42	156	25	65	40	160	23	62	39	170	19	59	40	211
7.5	28	73	45	161	27	70	43	159	25	66	41	164	23	63	40	174	19	60	41	216
8	28	73	45	161	27	70	43	159	25	67	42	168	23	63	40	174	19	61	42	221
8.5	28	74	46	164	27	70	43	159	25	67	42	168	23	64	41	178	19	62	43	226
9	28	74	46	164	27	71	44	163	25	68	43	173	23	65	42	183	19	62	43	226

Table 4.6.3E: Varying Strand Numbers of Second Continuous Example

This third continuous test illustrates an interesting trend that the addition of middle spans does not change the m value associated with the proposed equation. This is a very good sign that the proposed equation could be easily adopted as an alternative to the detailed method for all continuous members. The total change in rebar totals and percentages show signs of being relatively the same value regardless of the number or length of spans. Table 4.6.3F below summarizes all three tests.

Test	m value	# of Rebar Difference	% Difference
Continuous 1	2.5	38	90
Continuous 2	2	30	71
Continuous 3	2	25	100

Figure 4.6.3F: Summary of Three Continuous Tests

Chapter 5: Conclusions and Recommendations

5.1 Conclusions

The parametric study analyzing the difference between the detailed method and the proposed equation with regards to shear design reveled a lot about the behavior of the detailed method. According to the detailed method, V_c of a reinforced member is partially based on the loading it experiences. This makes designing using the detailed method rather tricky because as loads change, so does the strength of the member (ex. the changing compression face of a member along the length of a continuous beam). The detailed method can feel circular at times, and it is very easy to misunderstand one of the design steps when dealing with complex members. Having a design method that is independent of loading condition, like the proposed equation, would be far easier to use and understand. The research done for this thesis illustrates that it is indeed possible for a simplified shear design equation in the form of the current RC shear design equation to be available for complex members; however, there is still a lot of unknowns that need to be accounted for before making any applicable recommendations

As more prestressing strands were added to the various members, the value for the calibration term m for which the new equation was conservative along the entire length of the beam increased. This was expected and consistent across all the members. Transfer checks were accounted for to ensure no unrealistic sections were used; however, it is still possible that some of these sections might be unnecessary to include. Finalizing a m value for all members in all conditions would be difficult to determine right now, but a specified m value given the type of member, as well as the loading geometry is more realistic.

The difference between the overhang and the continuous beams were substantial. After looking at all five example geometries, these two types of members just behave so differently that right now it would not be wise to lump them together when deriving a new equation. Even an overhang specific equation would not be wise because of how different the two m values between the two overhang examples. Also, the length of the overhang can vary from beam to beam. Beams with large overhangs are much different than beams

with short overhangs. However, a continuous beam specific equation could be applicable, particularly with similar span lengths.

The continuous beams analyzed had much more consistent results from test to test. The proposed equation concrete strength graphs followed the same shape as the detailed method more closely than the overhang problems. With more data tests, and a further definition of the parameters for which the parametric study is performed, an applicable m value could be determined, and the proposed equation would then be a viable alternative to the detailed method.

5.2 Future Work and Recommendations

Based on all the research and data analysis that went into this thesis, the following statements are the recommendations for future work and implementation of the proposed equation.

First, the proposed equation is a viable option that works in principle, especially for continuous structures, but needs to have some bounds to ensure it is both accurate and conservative. Setting limits to calibrate the equation using a ratio of the prestressing force to the gross area of the section ($\frac{P}{A_g}$) should be explored further. The data from this thesis shows that the ratio of prestressing force to gross area of the section greatly affects the m value for the proposed equation.

Secondly, it seems that more work is needed in analyzing overhang structures. The concrete contribution graphs of the proposed equation did not follow the detailed method as closely in the overhang examples as it did in the continuous examples. Additionally, the ratio of support length to overhang length is likely a factor that greatly affects the results but was not explored for this thesis. Setting limits for the application of the proposed equation similar to the proposed prestressing force to gross area ratio will help in creating a more viable equation.

Next, it would be interesting to see how the m values change if the proposed equation was to only replace V_{ci} instead of the V_{ci} and V_{cw}. Most of the challenges that are associated with the detailed method come from determining the V_{ci} term. V_{cw} is rather

simple to calculate and doesn't depend on the loading of the structure. The m values would likely decrease, and the proposed equation would be an even more accurate alternative to the detailed method while still being significantly easier to determine.

Finally, given the promising prospect of simplifying the detailed method, it is our recommendations that ACI Committee 220 consider the modified shear equations listed below in the upcoming code cycle for implementation if additional work has been done since the completion of this thesis to further justify its validity.

$$V_c = (2\lambda\sqrt{f_c'} + \frac{N_u}{6A_g} + \frac{P}{mA_g})b_w d \qquad \text{Proposed Equation}$$

References

ACI Committee 318, “Building Code Requirements for Structural Concrete (ACI 318-19) and Commentary (ACI 318R-19),” American Concrete Institute, Farmington Hills, MI, 2019.

Belarbi, A., Kuchma, D. A., & Sanders, D. H. (2017). Proposals for New One-Way Shear Equations for the 318 Building Code History of Design Provisions. *Concrete International*, *39*(9), 29–32.

Bentz, E. C., & Collins, M. P. (2017). Updating the ACI Shear Design Provisions. *Concrete International*, *39*(9), 33–38.

Bondy, K. Dirk, and Bryan Allred. *Post-Tensioned Concrete 55Principles and Practice*. Lulu Publishing Services Inc., 13 Sept. 2019.

Cladera, A., Marí, A., Bairán, J.-M., Oller, E., & Ribas, C. (2017). One-Way Shear Design Method Based on a Multi-Action Model. *Concrete International*, *39*(9), 40–46.

Collins, Michael, and Kuchma, Daniel *ACI SR 96_S52 Collins and Kuchma How Safe are Our Large Lightly Reinforced Concrete Beams Slabs and Footings.pdf*. (n.d.).

CSA Committee A23.3, *Design of Concrete Structures: Structures (Design)- A National Standard of Canada*, Canadian Standards Association, Rexdale, Ontario, Canada, Dec. 1994, 199pp.

Frosch, R. J., Yu, Q., Cusatis, G., & Bažant, Z. P. (2017). A Unified Approach to Shear Design. *Concrete International*, *39*(9), 47–52.

Kang, T., Lee, D., Yerzhanov, M., and Ju, H. (2021). *ACI 318 Shear Design Method for Prestressed Concrete Members Attempt to improve applicability*. *4*.

Li, Yi-An, et al. “Shear Strength of Prestressed and Nonprestressed Concrete Beams.” *Concrete International*, vol. 39, no. 9, 1 Sept. 2017, pp. 53–57.

MacGregor, J. G., and Hanson, J. M., 1969, “Proposed Changes in Shear Provisions for Reinforced and Prestressed Concrete Beams,” ACI Journal Proceedings, V. 66, No. 4, Apr., pp. 276-288. Doi: 10.14359/7360

Park, H.-G., & Choi, K.-K. (2017). Unified Shear Design Method of Concrete Beams Based on Compression Zone Failure Mechanism. *Concrete International*, *39*(9), 59–63.

Perumalla, M., Yogeendra, R. H., & Laskar, A. (2022). Shear Tests on Post-Tensioned High-Strength Self-Consolidating Concrete I-Beams under Distributed Loads. *ACI Structural Journal*, *119*(1), 3–14.

Reineck, K.-H. (2017). Proposal for ACI 318 Shear Design. *Concrete International*, *39*(9), 65–70.

Saqan, E.I., and Frosch, R.J., “Influence of Flexural Reinforcement on Shear Strength of Prestressed Concrete Beams,” *ACI Structural Journal, V*. 106, No. 1, Jan.-Feb. 2009, pp. 60-68.

Schokker, Andrea. Prestressed, C., & Beams, C. (2018). *SECONDARY in Continuous Prestressed Concrete Beams Precast, Prestressed Concrete Bridge Girders Full-Depth Precast Concrete Bridge Deck Panels*. 34–35.

Solanki, H. T. (2007). Simplified modified compression field theory for calculating shear strength of reinforced concrete elements. *ACI Structural Journal*, *104*(3), 378–380.

Stevenson, D. (2006). A Unified Approach to Design. *Programming Language Fundamentals by Example*, *September*, 147–158.

Vecchio, F. J., and Collins, M. P., "The Response of Reinforced Concrete to In-Plane Shear and Normal Stresses," Publication No. 82-03, Department of Civil Engineering, University of Toronto, Toronto, Ontario, Canada, 1982.

Appendices

Appendix A: Example Problem for Shear Design (Detailed Method)

Given: 14 Prestressing Strands; f_c' = 4 ksi; DL = 2.2 klf; LL = 1 klf; f_{pu} = 270 ksi

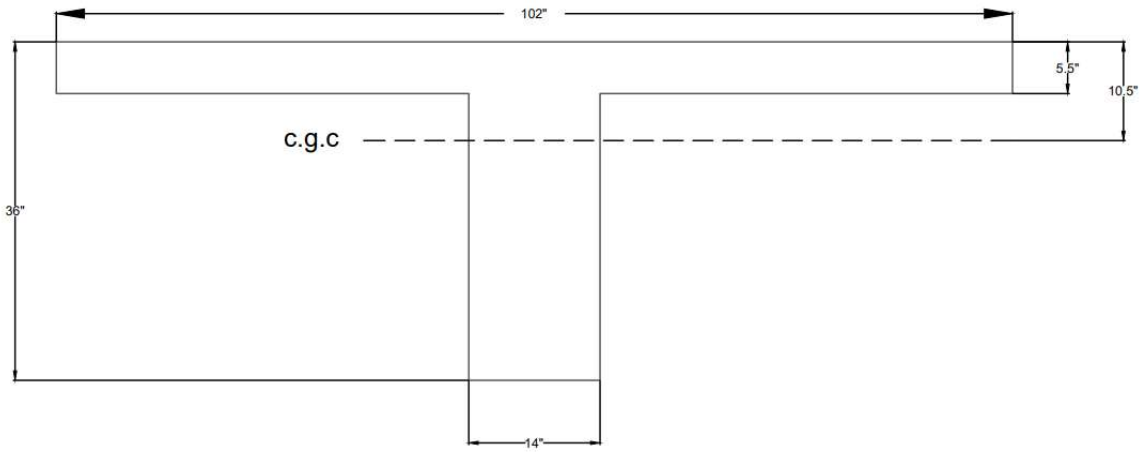

Figure A.1: Cross Section of Second Overhang Example

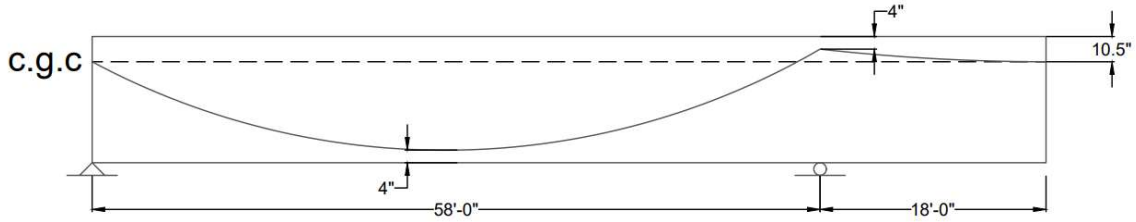

Figure A.2: Tendon Profile of Second Overhang Example

Calculated Beam Section Properties:

A = 1152 in^2

I = 128,703 in^4

St = 12,257 in^3

Sb = 5048 in^3

Solve for x = 10 ft

1. Determine Max Shear and Moment

Wu = 1.2(2.20 klf) + 1.6(1.0 klf) = 4.24 klf

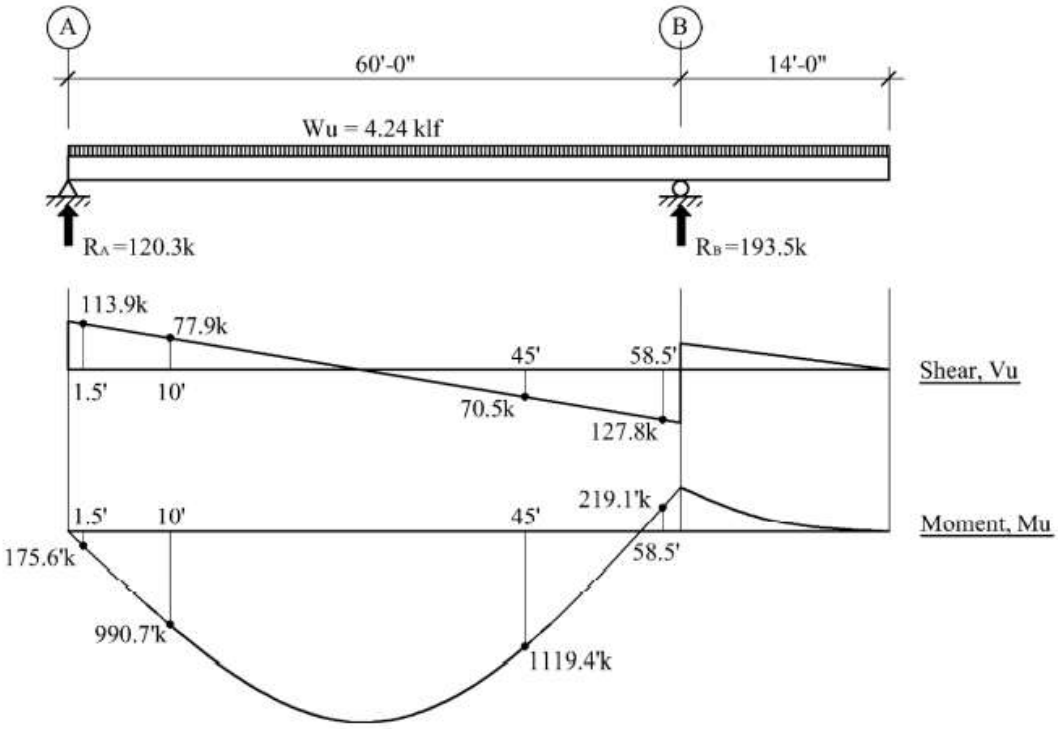

2. Determine Concrete Shear Contribution: V_{cn}

$$V_{cn} = \left(0.6\lambda\sqrt{f_c'} + 700\frac{V_u d_p}{M_u}\right) b_w d \qquad \text{ACI Eqn. 22.5.8.2(a)}$$

Where:

$1 \geq \frac{V_u d_p}{M_u}$ Eq A.1

$V_{cn} \leq 5\sqrt{f_c'}\, b_w d$ Eq A.2

@ x=10 ft

d_p = 23.17 inches; d = 28.8 inches

$\frac{V_u d_p}{M_u} = \frac{77.9\ kips * 23.17\ in}{(990.7\ kip*ft)*(12\frac{in}{ft})}$ = 0.152 < 1.0 Use 0.152

$V_{cn} = \frac{\left(\left(0.6\sqrt{4000}+700*(0.152)\right)*16\ in*28.8\ in\right)}{1000}$ = 66.4 kips

$V_{cn} \leq 5\sqrt{f_c'}\ b_w d$ => 66.4 kips < $\frac{5*\sqrt{4000}}{1000} * 16\ in * 28.8in$ = 145.7 kips

V_{cw} = 66.4 kips

3. Determine Concrete Shear Contribution: V_{ci}

$$V_{ci} = 0.6\lambda\sqrt{f_c'}b_w d_p + V_d + \frac{V_i M_{cre}}{M_{max}} \qquad \text{ACI 18-19 22.5.6.3.1}$$

Where:

$d_p > 0.8 * h$

$f_{pe} = \frac{P}{A} + \frac{M_{equiv}}{S_{tension}}$

$f_d = \frac{M_{dead}}{S_{tension}}$

$M_{cre} = S_{tension} * (6\sqrt{f_c'} + f_{pe} - f_d)$

@ x = 10 ft

V_d = 40.4 kips; M_d = 514.1 kip* ft

$f_{pe} = 0.324\ ksi + 372.7\ kips * \frac{23.17\ in - 10.5\ in}{5048\ in^3}$ = 1.259 ksi

$f_d = \frac{514.1\ kips*ft*12\frac{in}{ft}}{5048\ in^3}$ = 1.222 ksi

$M_{cre} = 5048\ in^3 * \frac{\frac{6\sqrt{4000}}{1000}ksi + 1.259\ ksi - 1.222\ ksi}{\frac{12in}{ft}}$ = 175.2 kips * ft

$V_{ci} = \frac{0.6\sqrt{4000}*16\ in*28.8\ in}{1000}\ kips + 40.4\ kips + \frac{77.87\ kips*175.2\ kips*ft}{990.7\ kips*ft}$ = 71.7 kips

4. Determine Concrete Shear Contribution: V_{cw}

$$V_{cw} = \left(3.5\lambda\sqrt{f_c'} + 0.3\ f_{pc}\right)b_w d_p + V_p \qquad \text{ACI 18-19 22.5.6.3.2}$$

@ x = 10 ft

$V_p = 0$

d_p = 28.8 in

$f_{pc} = \frac{372.7\ kips}{1152\ in^2}$ = 0.324 ksi

$V_{cw} = \left(3.5 * 1 * \frac{\sqrt{4000}}{1000} + 0.3 * 0.324\ ksi\right) 16\ in * 28.8\ in$ = 146.7 kips

5. Stirrup Design

$$S = \min\left(S_{(req'd)}, S_{(Max)}\right)$$

Where:

$V_c = \min(V_{ci}, V_{cw})$ = 71.7 kips

$V_{s(req'd)} = \frac{(V_u - \emptyset V_c)}{\emptyset}$

$S_{(req'd)} = \frac{A_v * f_y * d}{V_s}$

$S_{(Max)} = \min\left(0.75 * h, 24\right)$

@ x =10 ft

$V_c = \min(71.7, 146.7)$ = 71.7 kips

$V_{s(req'd)} = \frac{77.87\ kip \quad (0.75 * 71.7\ kips)}{0.75}$ = 32.17 kips

$S_{(req'd)} = \frac{2 * (0.11\ in^2) * 60\ ksi * 28.8\ in}{32.17\ \text{kips}}$ = 11.8 in

$S_{(Max)} = \min\left(0.75 * 36, 24\right)$ = 24

S = 11.8 in

Use 2 Legs #3 @ 11.8 in